# Synthesis and characterization of MDMA and development of field-deployable methods for its detection and quantification within Ecstasy tablets

J H HUSSAIN

2019

# Synthesis and characterization of MDMA and development of field-deployable methods for its detection and quantification within Ecstasy tablets

Jannat Hena Hussain

A thesis submitted in fulfilment of the requirements of Manchester Metropolitan University for the degree of Master of Science (by Research)

School of Science and the Environment

Manchester Metropolitan University

2019

# Abstract

The significant rise in NPS use, and particularly the use and misuse of 3,4-methylenedioxymethamphetamine (MDMA), has resulted in the need for a rapid, sensitive and field deployable method to facilitate its detection and subsequent quantification. Standards of MDMA and 4-methoxyamphetamine (PMA), a common adulterant encountered in tablets of MDMA, were prepared and characterised by $^{1}H$ and $^{13}C$ NMR, IR and mass spectrometry. 25 seized tablets (provided by Greater Manchester Police) were then analysed qualitatively by $^{1}H$ NMR and GC-MS, with acquisition times of 5 and 8 minutes respectively. All seized samples were found to contain MDMA only. Subsequent quantification, therefore, focused solely on quantifying the amount of MDMA present by primarily using $^{1}H$ NMR; GC-MS was employed as a complimentary technique in this regard. Quantification by $^{1}H$ NMR took 5 mins whereas acquiring the same MDMA concentration using GC-MS took 10 mins.

# Table of Contents

# List of Figures

# List of Tables

# List of Schemes

# Abbreviations

| | |
|---|---|
| ADHD | Attention deficit hyperactivity disorder |
| API | Active pharmaceutical ingredient |
| Ar | Aromatic benzene ring |
| $CaCO_3$ | Calcium carbonate |
| CAS | Chemical abstracts service |
| $CH_2$ | Methylene |
| COSY | Correlated spectroscopy |
| $d_6$-DMSO | Dimethyl sulfoxide-$d_6$ |
| DEPT | Distortion less enhancement by polarization transfer |
| DRD | Drug-related death |
| EMCDDA | European Monitoring Centre for Drugs and Drug Addiction |
| $Et_2O$ | Diethyl ether |
| FID | Free induction decay |
| GC-MS | Gas chromatography - mass spectrometry |
| $H_2O$ | Water |
| $H_2SO_4$ | Sulfuric acid |
| HMBC | Heteronuclear multiple bond correlation |
| HMQC | Heteronuclear multiple quantum coherence |
| ICH | International Conference on Harmonisation |
| IPA | Isopropyl alcohol |
| IR | Infrared spectroscopy |
| LAH | Lithium aluminium hydride |
| LoD | Limit of detection |
| LoQ | Limit of quantification |
| MDA | The Misuse of Drugs Act (1971) |
| MDMA | 3,4-methylenedioxymethamphetamine |
| MDMA.HCl | 3,4-methylenedioxymethamphetamine hydrochloride |
| Me | Methyl |
| MeOH | Methanol |

| | |
|---|---|
| MMU | Manchester Metropolitan University |
| MPTP | 1-methyl-4-phenyl-1,2,3,6-tetrahydropyridine |
| NaOH | Sodium Hydroxide |
| NMR | Nuclear magnetic resonance spectrometry |
| NPS | New psychoactive substances |
| $OCH_3$ | Methoxy |
| PAR | Peak area ratio |
| PMA | 4-methoxyamphetamine |
| PMA.HCl | 4-methoxyamphetamine hydrochloride |
| PMK | 3,4-methylenedioxyphenyl-2-propanone |
| PSA | The Psychoactive Substances Act (2016) |
| PVDF | Polyvinylidene difluoride |
| q-NMR | Quantitative NMR |
| $R^2$ | The coefficient of determination |
| RSD | Relative standard deviation |
| SIM | Single ion monitoring |
| SNR | Signal-to-noise ratio |
| UNODC | United Nations Office on Drugs and Crime |

# Acknowledgements

I would like to thank my supervisors, Dr Oliver B. Sutcliffe and Dr Ryan E. Mewis, for allowing me to join their remarkable team and allow me to complete this project, and also for providing me with constant guidance and feedback throughout this project and in the writing of this thesis. I would also like to thank all my friends and family for their constant support and encouragement, helping me keep focussed and always ensuring I am doing everything to the best of my ability.

# 1 Introduction

## 1.1 Drugs use (and abuse)

Drug abuse is the continued use of illegal drugs, or the misuse of prescription drugs that can lead to health issues and other negative consequences, and a serious public health problem that affects almost every community in some way. Each year drug abuse causes millions of serious illnesses or injuries and plays a role in many major social problems, such as driving under the influence, violence and stress. Drug abuse is thought to be an extremely complex disease and quitting usually requires time and upmost dedication,[1] due to the drugs changing the brain in ways that make the thought of having to go without drugs extremely stressful. Abused illicit drugs include cocaine, heroin and methamphetamine. They can alter a person's thinking and judgment, leading to health risks. Prescription drugs may also be abused and some of the most commonly abused medications are painkillers, specifically opioids. This is due to their side effect of inducing a euphoric high[2] and are usually only prescribed for more severe pains. Amphetamines are also commonly abused and are stimulants prescribed to help people with attention deficit hyperactivity disorder (ADHD),[3] a mental disorder causing the individual several social problems, such as difficulty paying attention, abrupt behaviour and hyperactivity. They are drugs which stimulate the cardiovascular and central nervous systems[4] and are recreationally used as they can cause a feeling of euphoria. This group of drugs may also be taken to increase wakefulness, improve focus, and enhance sociability.[5]

Stress is a well-known risk factor in the development of drug addiction,[6] and individuals exposed to stress are more likely to abuse alcohol and other drugs. Usually, the initial use of drugs is in the aim of finding relief and is the main cause of relapse.[7] However, there are several stages of drug use that may lead to addiction, and young people seem to move more quickly through the stages than do adults.[8] Drugs may be used for the first time as an experiment, done for recreational use, due to peer pressure, or simply because the user likes the way it makes them feel. Use usually depends on many factors such as how easy it is to get the drugs, location and

current trends. Recreational use is when users continue to use drugs to have fun and it becomes part of the individual's social life and use is seen as a 'normal' activity. At this point the user may still feel they have control over how regularly they use drugs. Regular, problematic or risky drug use is when the user begins losing motivation and worries about losing their drug source. They begin to believe that drug use is more important than all other interests, including studies, work and relationships and use of other, 'harder' drugs may increase.[8] Finally, dependency hits when the user has used drugs heavily or for a long period of time. This addiction means the individual is now unable to face daily life without their drugs and may be no longer able to control their use. As well as causing detrimental health effects, this may also cause emotional, psychological and social problems.

### 1.1.1 Drugs use (and abuse) in Manchester

Drugs are used by many different people and in many situations, and users tend to first be introduced to them in their youth. As a result, adolescents are more likely to take drugs than older people, with men twice as likely to take drugs than women.[9] Surveys from 2018 showed around 20% of young adults aged 16 to 24 in the UK had taken a drug in the last year,[10] which equates to around 1.2 million people, and around half of them had taken a drug in the past month. Also, the use of Class A drugs among younger adults has only been increasing since 2011/12 and is mainly driven by the increase in cocaine and ecstasy popularity and availability.

Young people (16–24 year olds) may begin taking drugs for various reasons, and trends in Class A drug use among young adults has shown a great increase in the last few years (Figure 1).[10] They may do it to try to 'fit in' with a group of friends, perhaps they have been offered drugs and feel pressured into taking them, or they know other people who use them or simply because they want to try something new and experience what it is like. However, it could also be used as a coping mechanism when affronted by difficult experiences or to deal with any problems they may be facing. In whatever circumstance drugs are used, they can still negatively impact the user

physically and/or mentally when used excessively or for a long period of time. This is when the chance of addiction is high and addiction can often be linked with additional mental health problems. This could affect the user's judgement and they may be more likely to take more drugs and engage in engaging in other types of risky behaviour.

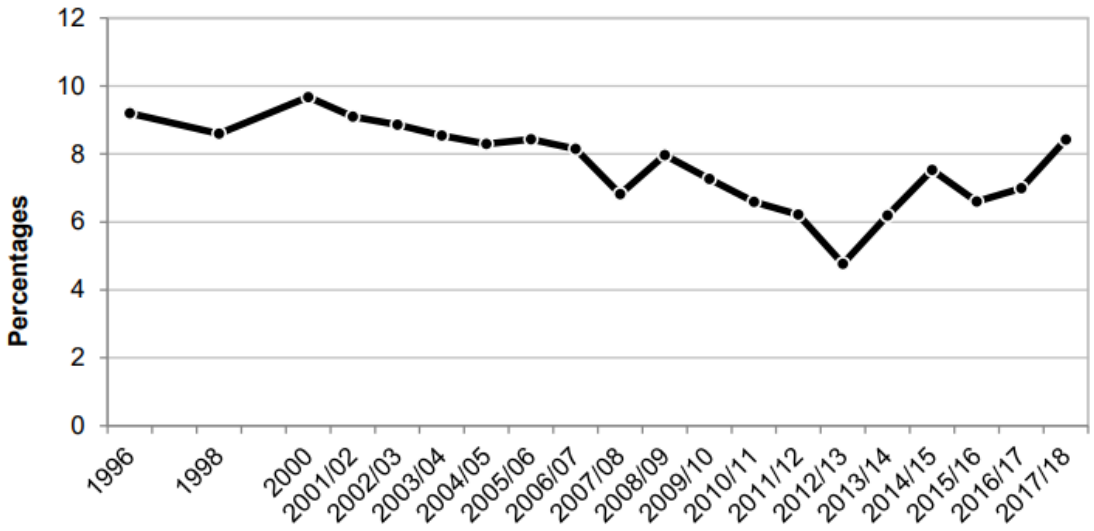


*Figure 1 Recent trends in Class A drug use by young adults*[10]

Rave and dance cultures were identified as an important part within the youth communities[9] and it was found that an increased level of drug use was associated with a higher frequency of visits to highly social settings such as pubs, clubs and festivals, such as the Parklife music festival in Manchester, UK. Here, drug tests are taking place on-site in order to find the nature of the drug and the amount in each sample.[11] Despite health warnings, people still take drugs, such as hallucinogenic and mood-enhancing drugs, in these settings to enhance their personal experience. They can be taken by the users own choice or due to peer pressure from friends or simply to look as though they are part of the society. Users who have visited clubs or festivals, consumed alcohol, or used another drug, were more likely to have used NPS in the last year than those who had not, and around half of all NPS users were young adults.[12]

It is known that illicit drug use is now a common feature of homelessness, and especially plays a role in the lives of young homeless people[13] and those exposed to stress and people who had first been exposed to drugs in their youth. Substance abuse is thought to be the cause of several mental and physical disorders are seen among the homeless. This leads on to mental illness being the reason they experience isolation when becoming homeless, feel humiliated and may believe their circumstances may never improve, and is ultimately one of the reasons the young homeless people death rate in the UK has risen,[14] with Manchester being reported as one of the major urban areas with the highest estimated numbers of deaths of homeless people. Suicide attempts were also significantly associated with homelessness, around 50% compared with around 20% of people who had not slept in the streets.[13] Undoubtedly, it was seen that areas in England with the higher deprivation and poverty had significantly more deaths of homeless people than the lesser disadvantaged areas.

Drug and substance misuse and addiction by a majority of the homeless community are usually methods for them of coping with stress caused by harassment,[15] high levels of illness, physical hardships and mental problems. This stress may be temporarily alleviated through drug use and users tend to get "geared up" on drugs such as heroin to cope and "ease the pain" from poor health and end up becoming addicted.[13] Users are unlikely to have the ability to abstain from taking these drugs as they believe for this self-medication to be a useful strategy. However, a large majority of reported illnesses attained by the homeless, whether mental and/or physical, could be traced back to the individual's drug use.[16] Cannabis generally seems to be the most popular choice, but stronger drugs, particularly the opiates, seemed to deal with the worst aspects of homelessness more effectively and evidently there were risks of transitioning to 'harder drugs'.[13]

## 1.2 The Misuse of Drugs Act

There are many medicinal substances which, if misused, have undesirable side-effects, including addiction,[17] mental illness and overdose. Controlled drugs (or substances) are drugs, which are considered dangerous or addictive in the UK and are therefore regulated by the law. The Misuse of Drugs Act (1971) [MDA] is the legislative apparatus, which is used to classify drugs and control their use and distribution. The act states all illegal drugs known in the UK and divides them into one of three classes[18] (A, B and C). Class A drugs (e.g. heroin, cocaine, ecstasy) represent those deemed most abusive and would pose the greatest danger (e.g. addiction), and so carry the harshest punishments whereas Class C (e.g. anabolic steroids, GHB and some tranquilisers) represents those thought to have the least capacity for harm, and so the Act demands more lenient punishment. Class B drugs (e.g. cannabis, ketamine, mephedrone) are not deemed as dangerous as those in Class A, however are more harmful than Class C so carry a heftier punishment. Certain Class B drugs can be reclassified to Class A if they have been prepared for administration by injection.

The maximum penalty for the possession of drugs are seven years imprisonment fine for Class A, five years for Class B and two years for Class C. The maximum penalty for the supply and possessions with intent to supply drugs, however, is much greater, with the penalties being life imprisonment for Class A and fourteen years imprisonment for Classes B and C.[18] All the imprisonment penalties carry a possible unlimited fine, depending on the crime. The Act was put in place to prevent the supply of controlled drugs and achieved this by posing a ban on the production, supply and possession of controlled drugs. Drug schedules are associated with the medicinal and therapeutic uses of a drug.[19] They range from schedule 1, which are drugs that are not used medicinally, to schedule 5, which are drugs which can be sold over the counter. Some Class A drugs, such has MDMA, have no therapeutic use and therefore cannot be lawfully possessed or prescribed and are controlled under the Misuse of Drugs Act within Schedule 1. However, although the Class A drug heroin has the potential for significant harm, it is used medically for pain relief and is a Schedule 2 substance, whilst mephedrone is a Class B (potentially less harmful) but has no medicinal value/usage and therefore is a Schedule 1 substance. Drug class is what the courts utilise in sentencing. In the 1990s the emphasis in UK government

policy was on reducing demand, whilst the focus in the 2000s was on harm reduction.[20] The MDA, therefore, must keep abreast of these developments in order to maintain its relevancy into which drugs are being misused and to which extent this is occurring.

## 1.3 NPS

New psychoactive substances (NPS), also known as 'designer drugs',[21] are a range of drugs that have been designed to imitate various prohibited drugs such as ecstasy, cocaine and cannabis. They are defined as 'Narcotic or psychotropic drugs that are not scheduled under the United Nations 1961 or 1971 Conventions, but which may pose a threat to public health comparable to scheduled substances'.[22] They are produced by altering chemical structures of the active functional groups found in traditional illicit drugs, hence allowing manufacturers to create new analogues. These drugs can be identified from the originals due to there being little to no history of them being used in medicinal circumstances. However, in the production and use of NPS there can be several side effects due to contaminants, this could have detrimental effects as the chemicals produced are not being tested thoroughly. For example, 1-methyl-4-phenyl-1,2,3,6-tetrahydropyridine (MPTP) (Figure 2, left) was found in prodine[23] (Figure 2, middle), which is an analogue of pethidine (meperidine, Figure 2, right) and has a similar effect to that of morphine. This then led to a number of injecting drug users to become affected by Parkinson's disease.[24]

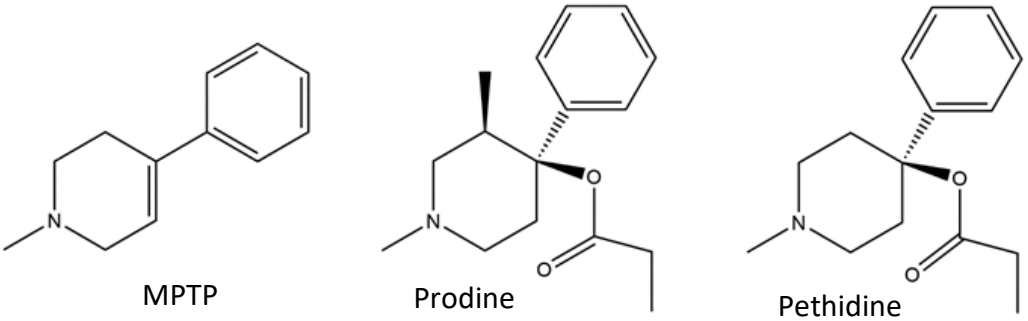


*Figure 2 Chemical structures of MPTP, Prodine and Pethidine*

The greatest rise in psychoactive substance use was in 1979 when the production designer drugs (synthetic opiates) started to emerge and use of illicit substances reached new heights,[25] and became apparent after a number of deaths due to drug poisoning and overdose. When street samples sold as heroin were seized by law enforcement officials and were tested, the results showed the substances were not of any known drug. It was identified as alpha-methylfentanyl, an analogue of fentanyl, an opioid that is like morphine but 50 to 100 times more potent.[26] Although the substances produced very similar effects to fentanyls, benzylpiperazines and cathinones (etc.), it was classified as a new substance and was not lawfully controlled.[25] This led to manufacturers of these drugs attempting to develop new chemical structures of these analogues to replace those that were banned, which resulted in the chemical structure constantly changing.[27] This was being achieved in illegal, unlicensed laboratories that were being used to synthesise the drugs that imitate the pharmacological effects of controlled substances to escape legislation controls[28] and to try to stay ahead of the law.

Due to new structures being constantly produced and released onto the drugs market, both principal drugs and their metabolites do not have reference standards in the chemical databases of drug analytic detection systems (such as GC-MS and NMR). This has led to increasing challenges for forensic and clinical laboratories in both the identification and quantification of psychoactive substances. Additional difficulties in analysis of these substances arise due to the complexity of some analytes, particularly when mixtures, due to high levels of adulteration put in place to attempt to disguise the drug. These developments led to the Psychoactive Substances Act (2016) [PSA] coming into force, which made it an offence to produce, supply or offer to supply any substances that produce a psychoactive effect within an individual. Penalties relating to this offence can subject an individual to a maximum sentence of 7 years' imprisonment and/ or a fine if they are caught offending.[29] However, simply being in possession of a psychoactive substance is not an offence unless it is within a custodial institution, such as prisons.

The Act came into play with the aim of working against the producers and sellers of NPS, aiming to reduce the numbers of dealers, shops and websites that supply these

products. It was hoped that subjecting producers and dealers to a sentence would emphasise the dangers of NPS and the number of people consuming them would decrease, therefore decreasing the death rate due to drug intoxication and poisoning. However, it was argued that the ban would only increase the death rates related to NPS, since the supply of these substances may be driven underground.[30] It was envisaged that this would decrease the research and knowledge relating to dosage, and due to the movement of the drugs becoming hidden, it would become more difficult to detect them.

### 1.3.1 The Chemistry of MDMA

3,4-methylenedioxymethamphetamine (MDMA, Molly or Ecstasy), shown in Figure 3, is a widely used Class A synthetic drug which acts as a stimulant and hallucinogen.[31] MDMA is prevalent on the recreational market, as it is commonly used at festivals, concerts and clubs. Due to its popularity, the number of both illegal and legal drug related deaths in England and Wales was 4,359 in 2018, the highest annual increase (16%) since the records began in 1993.[32] Ecstasy is often used to refer to MDMA in the tablet/capsule form, which is the most common way people use the drug.[33] On average, the effects of the drug when taken in this form can be felt around 45 minutes later and last an average of 3 hours[34] even though effects can be experienced up to days later. It has been determined that many ecstasy tablets can contain a variety of concentrations of MDMA along with several other drugs or drug combinations that can be harmful.[35]

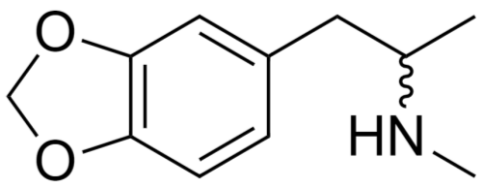


*Figure 3 Chemical structure of MDMA*

MDMA is predominantly used among young adults and adolescents. Social interactions often see the drug being abused at night clubs[36] and at festivals. This is due to the intoxicating effect of the drug. Other effects include increased extroversion, an enhanced sense of well-being[37] and increased empathy towards others.[38] However, the use of MDMA also has several health effects. Fatal overdoses can be potentially life threatening with symptoms including hypertension (high blood pressure), increased anxiety resulting in panic attacks and, in severe cases, unconsciousness and seizures.[39]

MDMA is readily absorbed from the digestive tract. Onset of action is within 30 minutes and the user's peak experience of the drug occurs after one to three hours.[40] With an elimination half-life of around 7 hours, the user may overdose and saturate themselves unknowingly. The drug causes the body to retain water[41] and due to its stimulant effects, it is associated with vigorous physical activity. The combination of use and effect causes dehydration[39] leading some people to drink large amounts of liquids. This can cause a sodium/electrolyte imbalance in the body that can lead to kidney failure[42] and swelling in the brain that could be fatal. Therefore, the aim to design a rapid detection and concentration determination system would be highly desirable. Regular use of MDMA has been known to cause sleep disturbances, depression, lack of appetite and heart disease.[43] However, more research is needed to understand the specific effects of regular MDMA use as no long-term assessments have yet been carried out.

Several pills known to be sold as ecstasy were tested and found to contain PMA (4-methoxyamphetamine, Figure 4), a compound with similar effects to ecstasy but with a higher toxicity and with higher lethality at lower doses.[44] This compound could also be used to adulterate tablets of MDMA, providing the desired effects with a smaller amount of compound. This was highlighted in a study from 2008, where a young male was admitted to a local hospital in Norway in a coma, and suffering from seizures, after taking the drug at a party.[45] He was diagnosed with PMA poisoning after apparently overdosing on the drug, having taken it in combination with MDMA. Adulteration of drugs in this way may be linked to drug-related deaths (DRDs) in the UK being at their highest levels since records began in 1993. There has been a

significant rise in the number of drug related deaths year on year, with the male drug poisoning rate, in England and Wales, increasing 18% from 2017 to 2018 whereas the female drug poisoning in 2018 was not statistically significant compared to 2017.[46] Most recorded cases of drug poisonings are because of drug misuse, and intoxications are an increasing public health problem for which no counteragents are clinically available.[47]

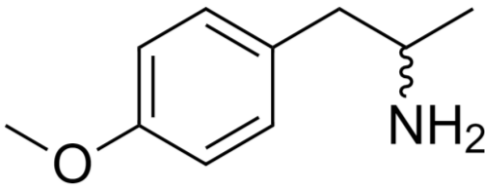


*Figure 4 Chemical structure of PMA*

Figure 5 shows the rate of male deaths related to drug poisoning has doubled since 1993 whereas the rate at which female deaths related to drug poisoning has increased at a much steadier rate. In studies, male drug abuse is usually set as the standard for addiction studies[48] due to comparative studies showing that drug addiction was more common among men than among women. In most cases, this is due to the ideology that males generally start using drugs at an earlier age and are more likely to use and abuse drugs more often and in larger amounts.[47]

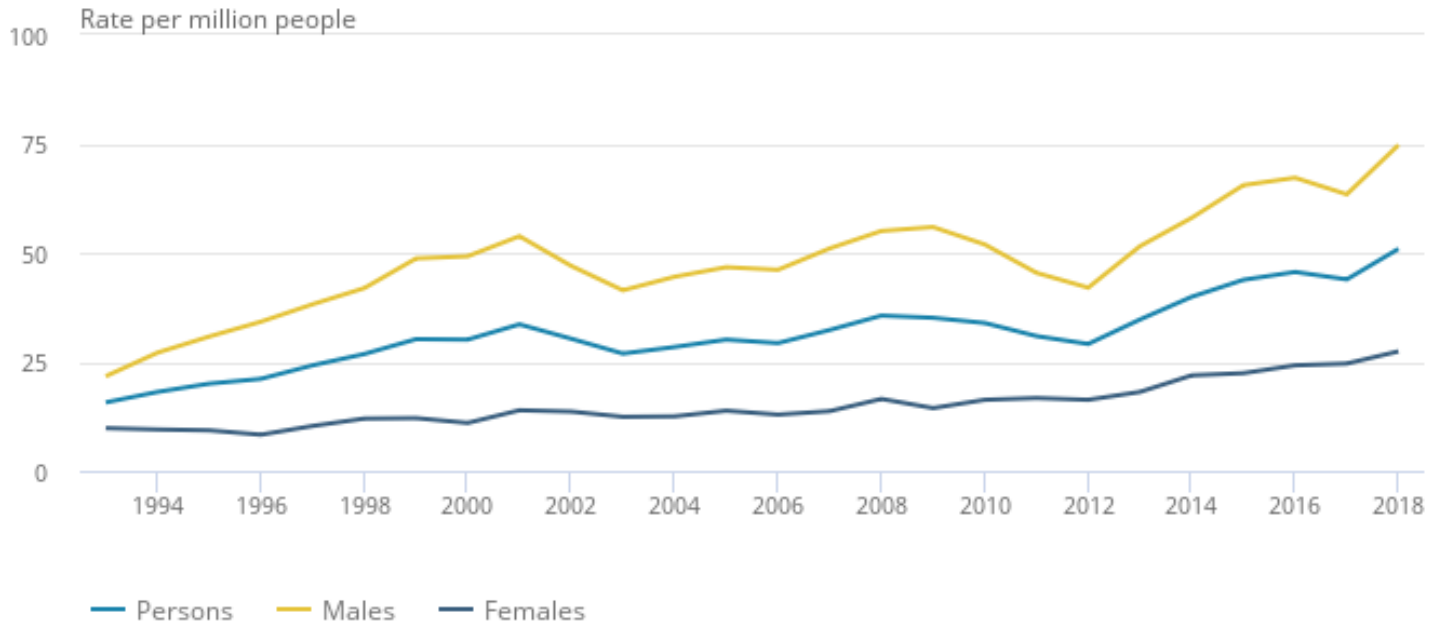


*Figure 5 Age-standardised mortality rates for deaths related to drug misuse, by sex, England and Wales, registered between 1993 to 2018*[35]

## 1.4 Drug identification and quantification

The importance of having a reliable technique to identify a drug, or drugs, within a sample is crucial since they provide valuable information on drug prevalence, undetectable movements, emergence of new drugs of abuse and to develop strategies to reduce the harms associated with substance misuse and abuse. Several methods currently employed to identify the drug present and subsequently quantify them include gas chromatography-mass spectrometry (GC-MS), nuclear magnetic resonance (NMR) spectrometry and infrared (IR) spectroscopy.

### 1.4.1 Gas Chromatography - Mass Spectrometry (GC-MS)

GC-MS is an analytical method which is currently the 'gold standard'[49] in the analysis of chemical compounds, this is due to this method being a simple and sensitive identification system for the detection of a broad spectrum of drugs. Several methods have been developed using this detection method already in the field of drug detection and analysis. For example, in 2000, a rapid detection method was developed for the identification of sympathomimetic amines in urine.[50] These are drugs, such as amphetamine, ephedrine and 3, 4-methylenedioxymethamphetamine, which effect certain characteristics of the sympathetic nervous system by stimulation the sympathetic nerves and produce physiological effects. Reports have been made of GC-MS being used for metabolic profiling; this simply refers to the detailed analysis of samples.[51]

The GC-MS detection method can be used to perform both targeted and non-targeted analyses,[51] where targeted analysis is when the analytes have been defined in advance, so they are known and are simply being detected. Non-targeted analysis allows detection of both known and unknown chemicals. Gas chromatography works on the principle that a mixture will separate into individual substances when heated. GC analysis was performed using an Agilent 7890B GC System (Agilent Technologies, Wokingham, UK) and data was acquired using the Agilent Mass Hunter Software

(Agilent Technologies, Wokingham, UK). The separation of molecules in a sample requires the use of a stationary phase, in this case a HP-5 capillary column (BGB Analytik, Switzerland) as it is non-polar and useful for the separation of semi-volatiles, drugs, alkaloids etc. Once the sample has been eluted from the column a temperature gradient is usually employed to an unknown sample in order to optimise the temperature programming. The quantification of the MDMA was obtained in SIM (single ion monitoring) mode in order to narrow down the window in which the molecular ions of the molecule is analysed. Ions were selected as a result of the fragment in the analysis, when MDMA was ionised by a beam of electrons, the molecule was broken into smaller fragment. This fragmentation process is specific to all molecules so allows identification and identification of unknown. In this investigation GC-MS was used as a comparative method used to validate the reliability of the development of the NMR method.

### 1.4.2 Infrared (IR) Spectroscopy

IR spectroscopy deals with the infrared region of the electromagnetic spectrum, which is a frequency of light with a longer wavelength and lower frequency than visible light. It works on the principle of vibrational spectroscopy which assesses the stretching or bending vibrations of molecules when they absorb photons of specific energy.[52] IR spectroscopy can be used as the solution to various issues revolving around drug identification. This includes its use in testing the purity of drug samples and observing interactions between the drug and various excipients, which act as a vehicle to deliver the drug into the system.

A method for the rapid verification of drugs was developed in 1991, focusing on the basis on IR spectroscopy.[53] Spectra for the samples were collected and the Agilent Mass Hunter software was used to identify the formula using a pre-installed library containing the chemical database, which is useful for obtaining reliable results with minimal operational use. Identification of additives were also achievable by subsequent data retrieval and searching against spectral libraries. This technique has also been reportedly used to identify counterfeit drugs in 2001,[54] where the spectrum of a sample was compared to a typical spectrum of the authentic drug, similar to the previous study. The samples used in this were said to contain the products Aspirina and Melhoral (both containing aspirin and used for pain relief). Statistical analysis of the samples allowed identification of the counterfeit samples from the genuine drugs, displaying the results clearly on a Coomans graph, which compares the distance of the results obtained from the sample to that of the model data for both drugs.

### 1.4.3 Nuclear Magnetic Resonance (NMR)

Nuclear Magnetic Resonance (NMR) is one of the most powerful and widely used analytical techniques in chemical research. It is a robust method, which can rapidly analyse mixtures at the molecular level without requiring a multitude of separation

and/or purification steps. In drug analysis, the usefulness of $^{1}H$ and $^{13}C$ nuclear magnetic resonance spectroscopy ($^{1}H$ and $^{13}C$ NMR) arises due to the fact that 1D and 2D data sets can be acquired, from which the atom connectivity can be established. This facilitates a route to establish the molecular structure of a compound. [55] A recent example of NMR being studied in drug identification was in 2011, where it was used to identify counterfeit drugs and detect drugs that were at a lower concentration than the active pharmaceutical ingredient (API),[56] in addition to other contaminants present. The application of $^{1}H$ NMR spectroscopy allowed for tablets of counterfeit drugs said to contain heparin (a blood thinner) and Viagra (used to treat erectile dysfunction) to be compared to spectra of genuine drugs. Resultantly, the compositions and chemical components of the counterfeits were determined.[57]

Alternatively, NMR is not only used in drug identification and quantification. For example, it can be used in drug discovery where its application can also be used in identifying how a substance interacts with biological macromolecules within an organism.[58] The goal of using NMR for this process is to justify the ligands have desirable interactions, so they can be subsequently developed into drugs. Due to the high sensitivity of the analytical method, even the weaker interactions can be detected, allowing for the screening of the smallest compounds and fragments.

Other uses for $^{1}H$ and $^{13}C$ NMR spectroscopy in drug analysis include:

- Identifying compounds present in unknown drug samples using a pre-installed library containing the chemical database as was done in 2018 where samples in drug-related case was qualitatively analysed using a desktop NMR spectrometer.[59]
- Quantifying the level of impurities as described in a 2014 study where a quantitative NMR (q-NMR) was developed and used an assessment measure for testing the purity of assays.[60]
- Quantifying the content of residual solvents as shows was possible in a study described in 2005, where they were found to be rapidly identified and quantified.[61]

- Identifying the isomeric composition of chemical components as in 1996 where the isomers of a nonsteroidal anti-inflammatory drug was separated in human urine.[62]
- Producing an assay of single drugs or drug compositions as shown in a 2019 study where q-NMR was used to assay different MDMA tablets seized from night-club venues in Bristol.[63]

# 2 Aims

The aims of this project are as follows:

- Investigate the application of bench-top nuclear magnetic resonance (NMR) spectroscopy for the rapid, sensitive and field deployable detection of controlled drugs (MDMA) and potentially extend this to new psychoactive substances (NPS).

- Build up the co-developed, patented technology between Manchester Metropolitan University (MMU) and Oxford Instruments and focus on the application of the technology to determine the presence (qualitative) and levels (quantitative) of MDMA present in seized samples (tablets) provided by law enforcement agencies.

- Development and validation of the method using International Conference on Harmonisation (ICH) and United Nations Office on Drugs and Crime (UNODC) guidelines and cross-validation of the method using an approved 'gold standard' method (in our case GC-MS).

- Provide data on the content of MDMA within seized samples, which can be used to further refine the field-deployed technology and inform law enforcement, healthcare professionals and front-line responders of potential and emerging drug/health threats to the public and vulnerable communities.

# 3 Experimental

All reagents were of commercial quality (Sigma-Aldrich, Gillingham, UK) and used without further purification. Solvents (Fisher Scientific, Loughborough, UK) were dried, where necessary, using standard procedures.[64] High field $^{1}H$, $^{13}C$, $^{1}H$-$^{1}H$ COSY, HMBC and HMQC NMR (50 mg/mL of MDMA in $d_6$-DMSO) spectra were acquired on a JEOL AS-400 (JEOL, Tokyo, Japan) NMR spectrometer operating at a $^{1}H$ resonance frequency of 400 MHz and referenced to the residual solvent peak (δ = 2.50, $d_6$-DMSO). Low field $^{1}H$ NMR spectra were acquired on an Oxford Instruments bench-top Pulsar® NMR spectrometer operating at a $^{1}H$ resonance frequency of 60 MHz and referenced to the residual solvent peak (δ = 2.50, $d_6$-DMSO). Infrared spectra were obtained in the range 4000 – 400 $cm^{-1}$ using a Thermo Scientific Nicolet iS10ATR-FTIR instrument (Thermo Scientific, Rochester, USA). GC-MS analysis was performed using an Agilent 6850 GC and a MS5973 mass selective detector (Agilent Technologies, Wokingham, UK). The mass spectrometer was operated in the electron ionisation mode at 70 eV. Separation was achieved with a capillary column (HP5 MS, 30 m Å~ 0.25 mm i.d. 0.25 µm) with helium as the carrier gas at a constant flow rate of 1.0 mL/min. The oven temperature programme started at 50 °C, increased at 30 °C/min and was held at 290 °C for 2 minutes. A 1 µL aliquot of the samples (qualitative analysis, calibration standards and test solutions) were injected (manually) with a split ratio of 20:1. The injector and the GC interface temperatures were both maintained at 280 °C and 290 °C respectively. The MS source and quadrupole temperatures were set at 230 °C and 150 °C, respectively. Mass spectra were obtained in full scan mode (50 – 550 amu).

## 3.1 MDMA Synthesis

Racemic MDMA.HCl was prepared in house *via* the sodium borohydride method[65]
Yield = 68%, MP = 208 – 209 °C.

**3,4-methylenedioxymethamphetamine:** $^{1}$H NMR ($d_6$-DMSO, 400 MHz, 298 K), δ (ppm) = 9.25 (s, 2H, N-$H_2$), 6.87 (d, $^{4}J_{HH}$ = 1.43 Hz, 1H, Ar-H), 6.85 (d, $^{3}J_{HH}$ = 7.90 Hz, 1H, Ar-H), 6.70 (dd, $^{4}J_{HH}$ = 1.43 Hz and $^{3}J_{HH}$ = 7.90 Hz, 1H, Ar-H), 5.99 (s, 2H, $O_2$C-$H_2$), 3.25 (m, 1H, C-H), 3.11 (dd, $J_{HH}$ = 13.15 Hz and $J_{HH}$ = 4.28 Hz, 1H, C-$H_2$), 2.58 (dd, $J_{HH}$ = 13.15 Hz and $J_{HH}$ = 9.96 Hz, 1H, C-$H_2$), 2.52 (s, 3H, C-$H_3$), 1.09 (d, $^{3}J_{HH}$ = 6.52 Hz, 3H, C-$H_3$); $^{13}$C NMR ($d_6$-DMSO, 400 MHz, 298 K), δ (ppm) = 101.4 (1C, $O_2$**C**$H_2$), 147.9 (1C, Ar**C**O), 146.5 (1C, Ar**C**O), 110.0 (1C, Ar**C**H), 130.9 (1C, Ar**C**$CH_2$), 122.9 (1C, Ar**C**H), 108.8 (1C, Ar**C**H), 38.4 (1C, ArC**C**$H_2$), 55.8 (1C, $CH_2$**C**HNHC$H_3$), 30.1 (1C, NH**C**$H_3$), 15.4 (1C, CHNH**C**$H_3$); IR (ATR-FTIR), ($cm^{-1}$): 2946 (N-H), 1489 (ArC=C), 1033 (Ar-O-$CH_3$), 798 (C-H).

## 3.2 PMA Synthesis

Racemic PMA.HCl was prepared in house, using a reported adaptation of the synthesis reported by Liu *et al.*[66] and produced an off-white crystalline powder. A solution of anisaldehyde (27.2 g, 199.78 mmol) and nitroethane (18.0 g, 239.78 mmol) in benzene (300 mL) was treated with cyclohexylamine (2.0 mL, 17.43 mmol) and refluxed until $H_2O$ ceased to accumulate. After the solvent was removed, the oily residue was cooled and crystallized producing 1-(4-methoxyphenyl)-2-nitropropene as yellow crystals, which were used without further purification. A suspension of lithium aluminium hydride (32 g, 843.21 mmol) in anhydrous $Et_2O$ (1 L) was stirred and crude 1-(4-methoxyphenyl)-2-nitropropene (32.6 g, 168.74 mmol) in $Et_2O$ was added at a steady rate. Reflux was then continued for 48 hours. The reaction mixture was cooled, and dilute $H_2SO_4$ was added. A solution of potassium sodium l(+)-tartrate tetrahydrate (700g, 2481.39 mmol) in $H_2O$ (600 mL) was added, along with 25% NaOH which was added until the pH was brought to >9. This aqueous phase was extracted with $CH_2Cl_2$ (3 x 200 mL). The oil produced was dissolved in isopropyl alcohol (100 mL), neutralized with concentrated HCl, and then diluted with anhydrous $Et_2O$ (300 mL) to provide white crystals of 4-methoxyamphetamine hydrochloride (PMA). Yield = 271.4 mg (14%) $^{1}$H NMR ($d_6$-DMSO, 400 MHz, 298 K), δ (ppm) = 8.17 (s, 2H, N-$H_2$), 7.11 (dd, $^{3}J_{HH}$ 8.42 Hz, 2H, Ar-H), 6.85 (dd, $^{3}J_{HH}$ 8.42 Hz, 2H, Ar-H), 3.68 (d, 3H, OC-$H_3$),

3.26 (s, 1H, C-H), 2.94 (dd, $^{2}J_{HH}$ = 13.38 Hz and $^{3}J_{HH}$ = 4.95 Hz, 1H, C-H), 2.55 (dd, $^{2}J_{HH}$ = 13.38 Hz and $^{3}J_{HH}$ = 9.20 Hz, 1H, C-H), 1.05 (d, $^{3}J_{HH}$ = 8.00 Hz, 3H, C-$H_3$); $^{13}$C NMR ($d_6$-DMSO, 400 MHz, 298 K), δ (ppm) = 55.6 (1C, O**C**$H_3$), 114.5 (2C, Ar**C**H), 158.6 (1C, Ar**C**O), 130.8 (2C, Ar**C**H), 129.2 (1C, Ar**C**$CH_2$), 39.7 (1C, ArC**C**$H_2$), 48.7 (1C, $CH_2$**C**H$NH_2$), 17.9 (1C, CH$NH_2$**C**$H_3$); IR (ATR-FTIR), ($cm^{-1}$): 2914 (N-H), 1508 (ArC=C), 1032 (Ar-O-$CH_3$), 807 (C-H); MP = 208-209 °C.

## 3.3 MDMA NMR Calibration

MDMA (5 – 300 mg/mL) in $d_6$-DMSO calibration standards were produced by dissolving the weighed amounts of MDMA in $d_6$-DMSO (1 mL). The $^{1}$H NMR spectrum of the MDMA sample was acquired using a Pulsar® benchtop NMR spectrometer (Oxford Instruments, Abingdon, UK). A concentration vs. integral graph was plotted for each of the 3 H environments decided to be the focus of in this investigation: Ar, $CH_2$ and Me. The chemical shift regions for each environment is [6.918 ppm to 6.444 ppm], [6.036 ppm to 5.768 ppm] and [1.191 ppm to 0.669 ppm] respectively.

## 3.4 MDMA GC-MS Calibration

Stock solutions of MDMA.HCl (100 µg/mL) in MeOH (stock solution A), and eicosane (100 µg/mL) in MeOH (stock solution B) were prepared respectively. Five GC-MS calibration standards were produced all containing the same amount of the eicosane (10 µg/mL) and varying amounts of the MDMA.HCl solution: 5, 10, 15, 20 and 25 µg/mL. The samples were run in SIM mode, using selected ions (m/z = 58.10, 77.00 and 135.10) for quantification, and each solution was injected six times.

## 3.5 NMR Simulated Samples

Simulated mixtures, of MDMA and calcium carbonate ($CaCO_3$), were made up using $CaCO_3$ (0.7790 g) and MDMA (2.0083 g) weighed using an AB104-S analytical balance (Mettler Toledo, Leicester, UK). The powders were homogenised using a pestle and mortar and 6 samples of approximately 0.46 g were extracted to determine the MDMA concentration by dissolving in $d_6$-DMSO, filtering through a 0.45 um PDVF (polyvinylidene difluoride) syringe filter (Whatman, Sigma-Aldrich, Dorset, UK) directly into an NMR tube. The sample was then analysed. The concentrations were determined by comparing the integrals to the concentration vs. integral graph produced for each integral region: Ar, $CH_2$ and Me.

## 3.6 Unknown Samples Analysis By NMR

Each of the 25 seized tablet samples of unknown and purported to be MDMA (ecstasy) identity were obtained from Greater Manchester Police *via* the MANchester DRug Analysis & Knowledge Ex-change (MANDRAKE) partnership and were stored and analysed in accordance with the UK Misuse of Drugs Act (1971) and Misuse of Drugs Regulations (2001). The samples were collected over the period August 2018 – August 2019.

All of these samples were supplied in their solid, bulk, forms and were photographed (example shown in Figure 6). They were accurately weighed using an AB104-S analytical balance (Mettler Toledo, Leicester, UK), thoroughly homogenised using a pestle and mortar and added into a glass vial. 30 mg of the sample was removed to be used for GC-MS measurements. $d_6$-DMSO (1 mL) was pipetted into the vial using an eVol® XR digitally controlled positive displacement dispensing system (Trajan, Victoria, Australia) with a 1 mL eVol® syringe and then filtered through a 0.45 µm PVDF (polyvinylidene difluoride) syringe filter (Whatman, Sigma-Aldrich, Dorset, UK) directly into an NMR tube.


*Figure 6 Representative photograph of seized pink bear MDMA tablets*

The $^{1}$H NMR spectrum of the MDMA samples was acquired in four scans and a relaxation delay of 60 s was utilised. The temperature of the probe was calculated to be 308.5 K by measuring the separation (in Hz, Δδ) between the $CH_2$ and OH signals of neat ethylene glycol and implementing the equation T [K] = 466.5 - 102.00 Δδ.[67] After the NMR sample tube had been inserted, an automated procedure began whereby the instrument would lock on to the deuterated signature of DMSO (thus used as a chemical shift reference) before acquiring the $^{1}$H NMR spectrum. The collection of sample NMR data and the subsequent analysis took approximately 5 minutes.

Following acquisition, the data was processed in MNova (Mestrelab Research, Santiago de Compostela, Spain) using an automated script file. The processed free induction decay (FID) file was then analysed using a pattern recognition algorithm,[67] developed in-house using Matlab (The Mathworks Inc, Cambridge, UK). The spectrum was processed using a 1 Hz exponential in the $T_1$ direction and phased accordingly. Integrals of the aromatic, methylene and N-$CH_3$ groups were then obtained which had been referenced against a standard containing 100 mg of MDMA in 1 mL deuterated DMSO. Using the calibration plots as outlined in section 4.5, the amount of MDMA was determined. Each experiment sample was collected five times. The average integral is reported for each of the three resonances considered, with a relative standard deviation (%RSD) calculated from the five different acquisitions.

## 3.7 Unknown Samples GC-MS

Tablet samples were crushed into a powder using a pestle and mortar, and two masses of each sample were taken at 10% of the powder weight. The sample was dissolved in 100 mL MeOH and filtered using a fluted filter paper in to a beaker. 10 mL of the tablet sample was extracted in to a 100 mL volumetric flask and 10 mL of eicosane solution (0.5 mg/mL of eicosane in MeOH) was added. The sample was then made up to 100 mL with MeOH to give a dilution factor of 1:10 and 0.5 µL of this solution was analysed on the GC with two injections following the calibration series which was injected three times. The three ions monitored were at m/z = 58.10, 77.00 and 135.10 (for MDMA) and 43.00, 57.00 and 71.00 (for eicosane). Using the Qualitative Analysis Agilent Mass Hunter Software, the retention times for MDMA and eicosane appeared to be at 5.634 and 7.234 minutes respectively. A generalised GC method was used, and the chromatogram was obtained using a concentration gradient initiating at 50 °C and increasing at a steady rate of 30 °C / min until the temperature rose to 290 °C. This temperature was then maintained for 2 minutes.

# 4 Results and Discussion

## 4.1 MDMA Synthesis

MDMA synthesis was carried out using the sodium borohydride method.[65] The synthesis began using the plant oil safrole (1-allyl-3,4-methylenedioxybenzene) and was oxidised into a ketone, PMK (3,4-methylenedioxyphenyl-2-propanone). From this compound, three routes can be utilised by which the MDMA base can be synthesised. In this instance, MDMA was synthesised by reductive amination, as shown in Scheme 1**Error! Reference source not found.** using route A.[65] The MDMA base was then converted to the HCl salt.

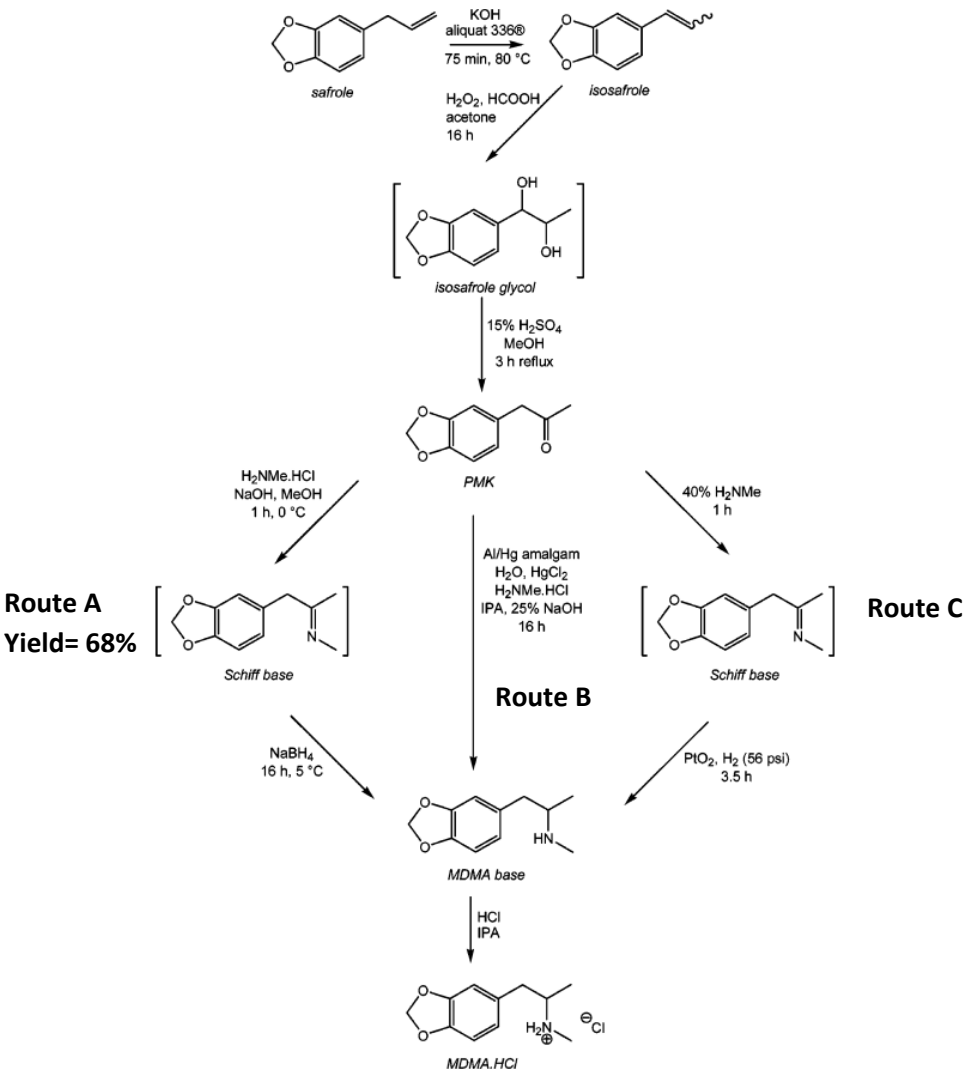


*Scheme 1 Synthetic pathway from safrole to MDMA.HCl[65]*

MDMA was then fully characterised using NMR, GC-MS and IR. The 50 mg/mL $d_6$-DMSO sample was used to carry out the analysis and the structural configuration was determined.

## 4.2 MDMA Characterisation

### 4.2.1 NMR Characterisation

The supplied sample of MDMA was analysed using $^{1}H$ and $^{13}C$ NMR spectroscopy to ascertain its analytical purity. A combination of 1D and 2D methods were employed for complete structural elucidation.

MDMA has 9 $^{1}H$ NMR resonances, and therefore 9 unique $^{1}H$ NMR environments (chemical structure shown in Figure 7 along with atom numbering system), accounting for 16 proton nuclei. This is reflected in the $^{1}H$ NMR spectrum for the compound (Figure 8). The two ammonium protons at position 10 are observed at 9.25 ppm as a broad singlet; this is due to them exchanging in the ammonium salt form. The aromatic protons located at position 6 appears as a doublet of doublets at around 6.70 ppm. This is due to the proton at positon 6 having a $^{4}J_{HH}$ coupling of 1.43 Hz and a $^{3}J_{HH}$ coupling of 7.90 Hz to protons 4 and 7 respectively. Protons 4 and 7 both appear as doublets centred at 6.87 and 6.85 ppm resepectively.

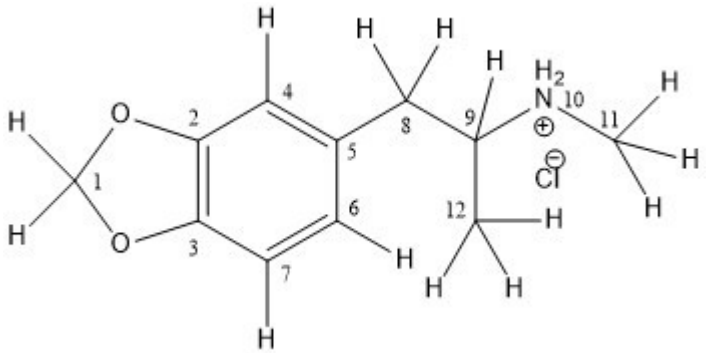


*Figure 7 Chemical structure of MDMA HCl salt with atom numbering shown*

The two protons located at position 1 are observed at 5.99 ppm as a singlet. The peak sits in a relatively low-field position due to the protons being deshielded by the oxygens bound to the carbon centre thus increasing the frequency.

There is a chiral centre located at position 9 in the structure on MDMA containing a single proton. This is presented as a multiplet at approximately 3.25 ppm with a $^{3}J_{HH}$ coupling of 6.52 Hz from the methyl and $^{3}J_{HH}$ couplings of 13.15 Hz and 4.26 Hz at 3.11 ppm, and couplings of 13.15 Hz and 9.96 Hz at 2.58 ppm from the methylene. The cross-peaks in the $^{1}H$-$^{1}H$ COSY NMR spectrum (Figure 9) reflect this observation.

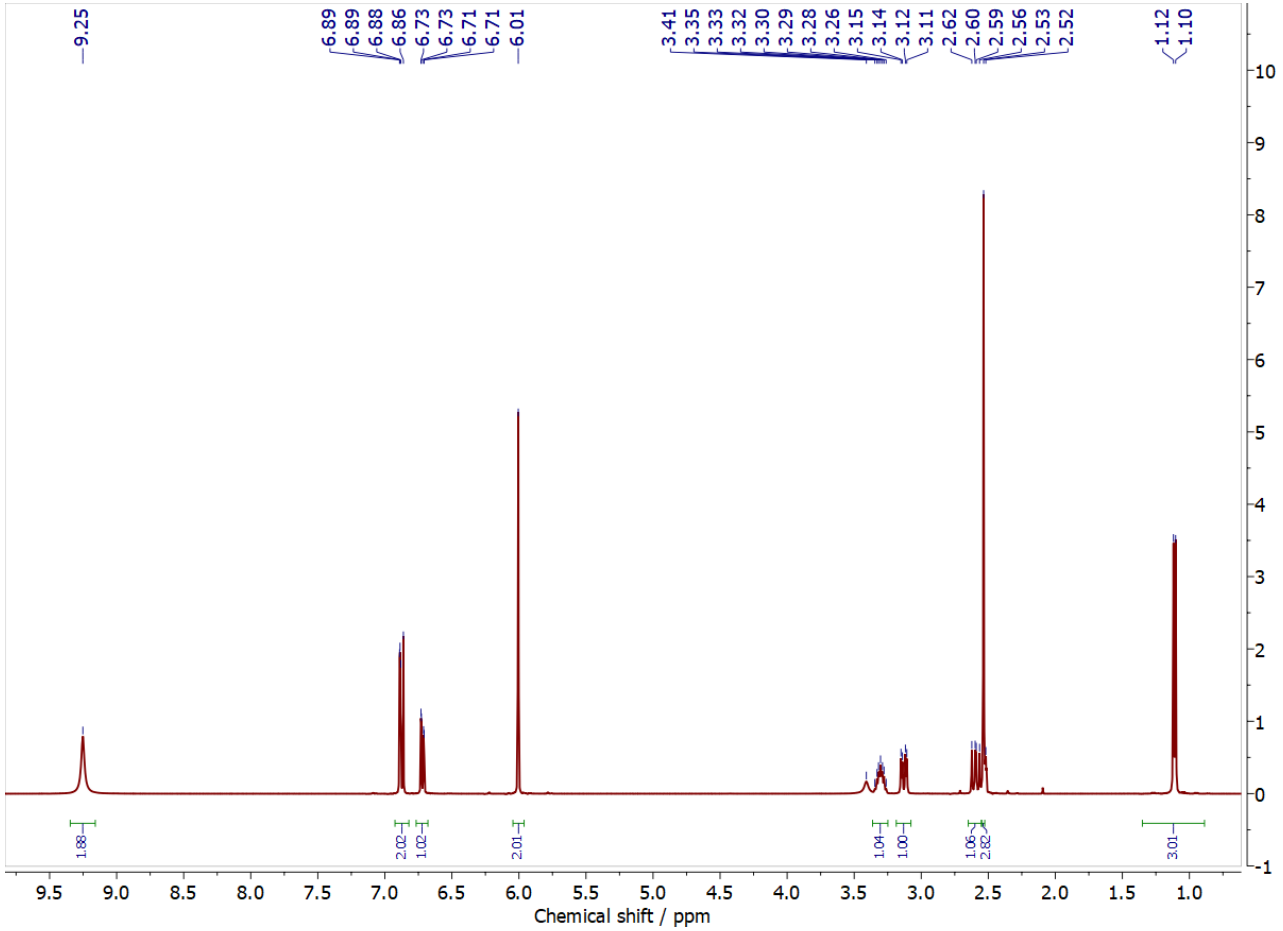


*Figure 8 $^{1}H$ NMR spectrum of MDMA collected in $d_6$-DMSO*

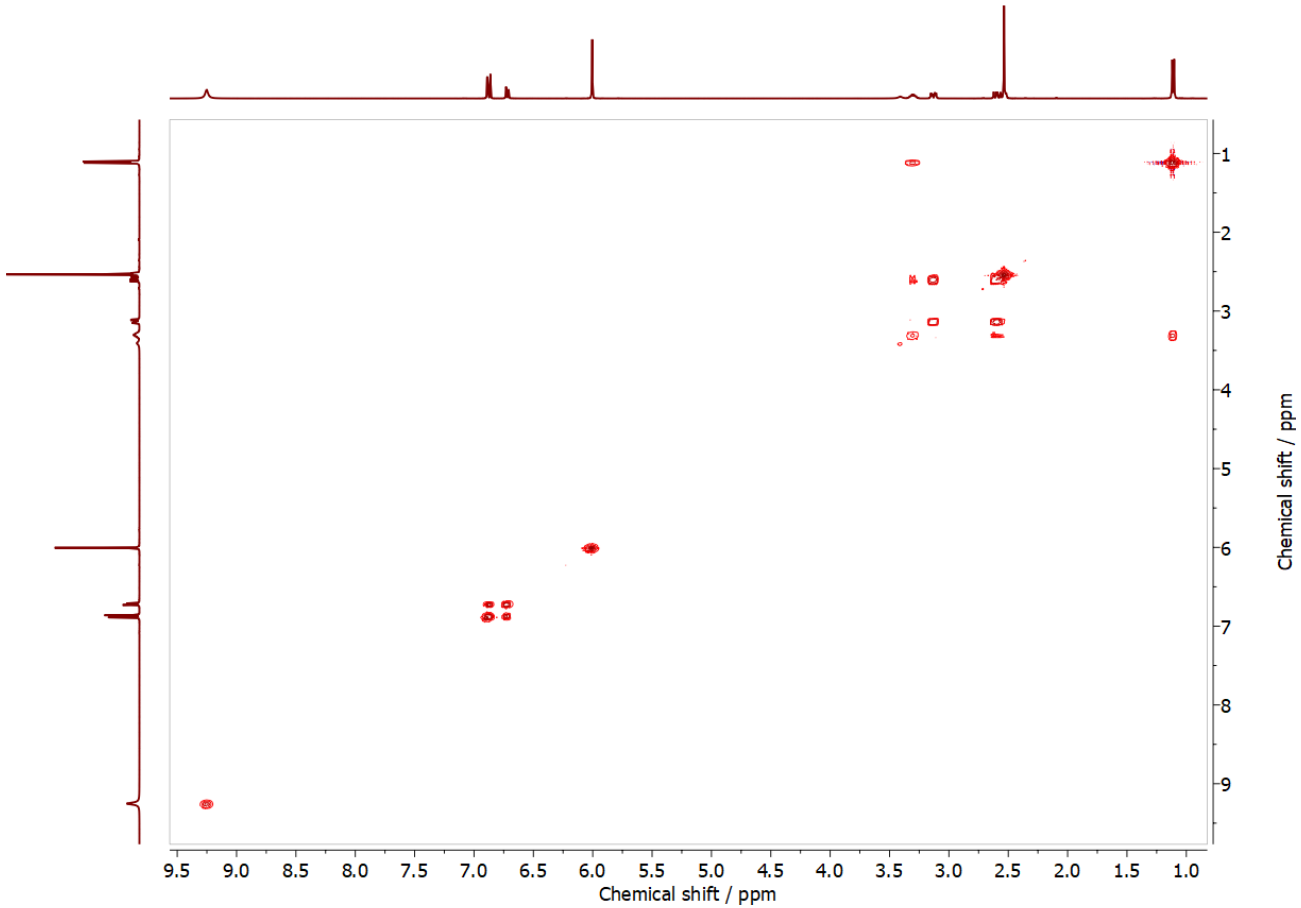


*Figure 9 $^{1}H$-$^{1}H$ COSY NMR spectrum of MDMA collected in $d_6$-DMSO*

The methylene group with two protons at position 8 is separated into two individual doublets at 3.13 ppm and 2.59 ppm that have $^{3}J_{HH}$ couplings of 4.26 Hz and 9.92 Hz respectively. The methyl group attached to the ammonium centre containing three protons at position 11 are observed at 2.52 ppm as a singlet. This peak does not show any coupling. The three protons on the methyl group at position 12 are the most shielded in the spectrum and are present at 1.11 ppm as a doublet with a $^{3}J_{HH}$ coupling of 6.52 Hz. This is due to there being the greatest amount of shielding of the protons, so they sit at the highest-field position on the spectrum.

The $^{13}C\{^{1}H\}$ NMR spectrum of MDMA (Figure 10) reveals that the structure contains 11 unique carbon environments. In order to be able to identify which peaks are associated with the corresponding carbons, a DEPT-135 NMR spectrum of MDMA (Figure 11) was collected in order to simplify this. This is due to the quaternary carbons at positions 2, 3 and 5 on the structure (Figure 7) at 147.41 ppm, 146.04 ppm and 130.45 ppm are no longer observed. The carbon atoms containing one (tertiary) or three protons (primary) are positive (point up) and the carbon atoms containing only two protons (secondary) are negative (point down).

The two carbons at positions 1 and 8 both contain two protons, so are therefore secondary carbons. The methylene at position 1 is more de-shielded than the one at position 8, therefore will have a higher chemical shift and is seen at 100.9 ppm. Carbon 8 must therefore appear at 37.9 ppm. The three carbons on the aromatic ring at positions 7, 6 and 4 on the structure all contain one proton and are tertiary. They appear at 122.4 ppm, 108.3 ppm and 109.5 ppm respectively. The two methyl groups at positions 11 and 12 contain 3 protons (primary) and will sit at the lowest chemical shifts. Due to the carbons at position 11 being more de-shielded, they will lie most up-field at the lowest frequency so therefore is assigned the peak at 141.9 ppm. This leaves the peak at 29.5 ppm being assigned to position 12. Finally, the chiral centre and tertiary carbon at position 9 is observed at 55.4 ppm in the DEPT-135 NMR spectrum.

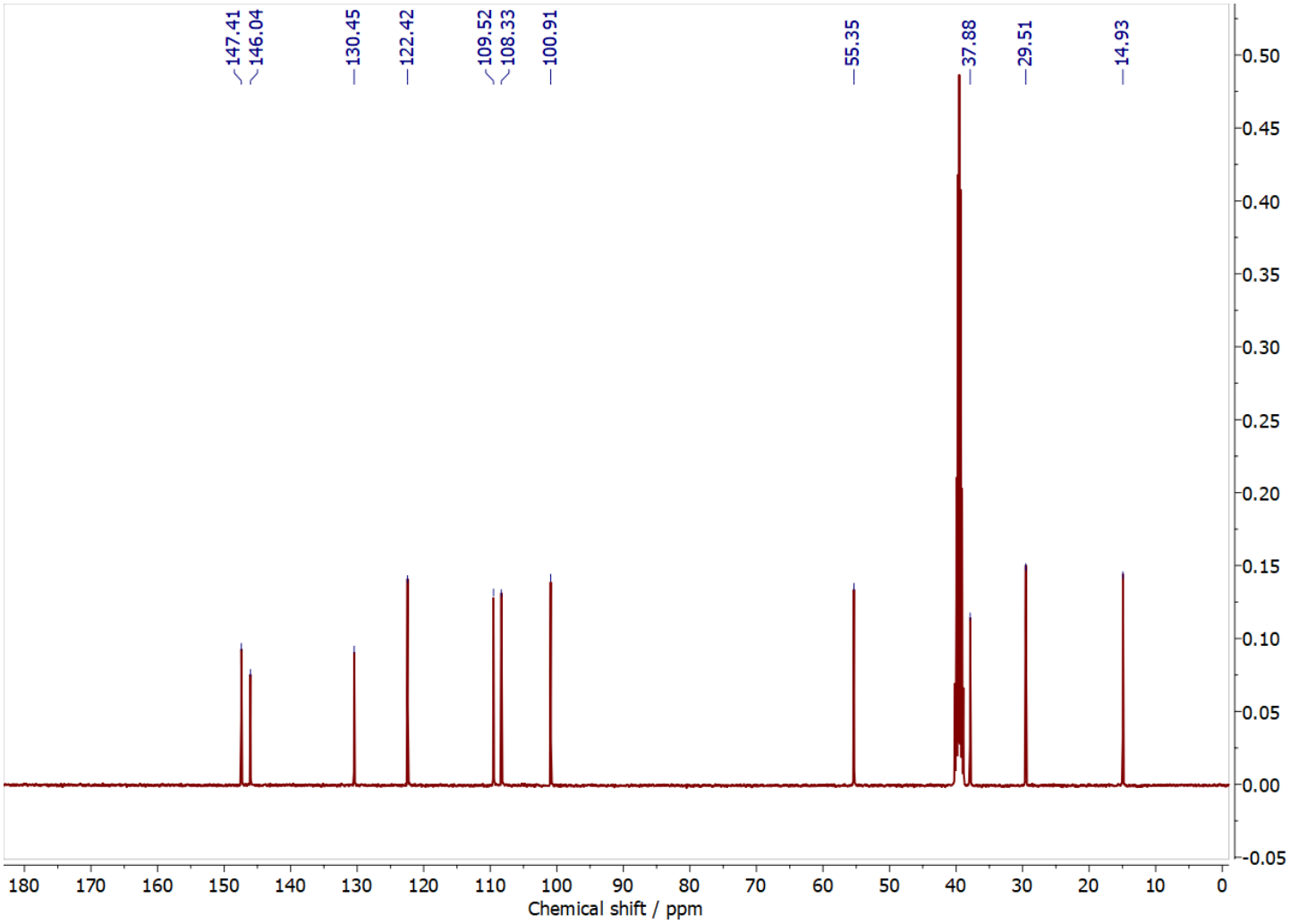


*Figure 10 $^{13}C\{^{1}H\}$ NMR spectrum of MDMA collected in $d_6$-DMSO*

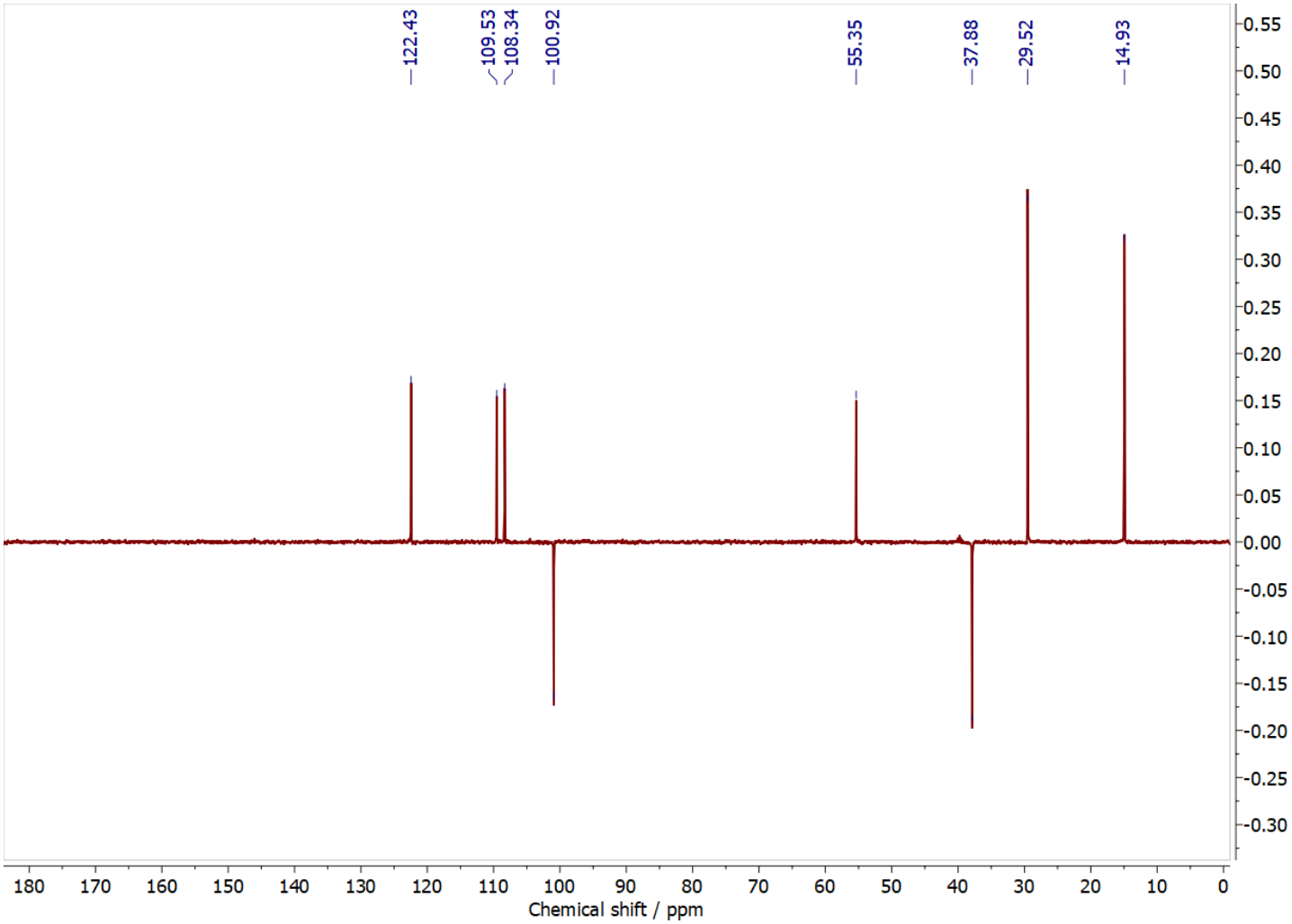


*Figure 11 DEPT-135 $^{13}C\{^{1}H\}$ NMR spectrum of MDMA collected in $d_6$-DMSO*

The $^{1}H$-$^{13}C$ HMQC NMR spectrum of MDMA (Figure 12) was used to determine the connectivity of the protons and carbons using the $^{1}H$ NMR spectrum and $^{13}C\{^{1}H\}$ NMR spectrum. From the HMQC spectrum it is seen that the proton located on position 6 (Figure 7) is connected to the carbon at position 6 at 55.4 ppm. On inspecting the spectrum further, it is seen the protons located at position 8 are connected to the carbon at position 8 at 37.9 ppm. In addition, using the spectrum it is clear to identify the three peaks at 147.4 ppm, 146.0 ppm and 130.5 ppm were most certainly quaternary as they are not directly connected to a proton.

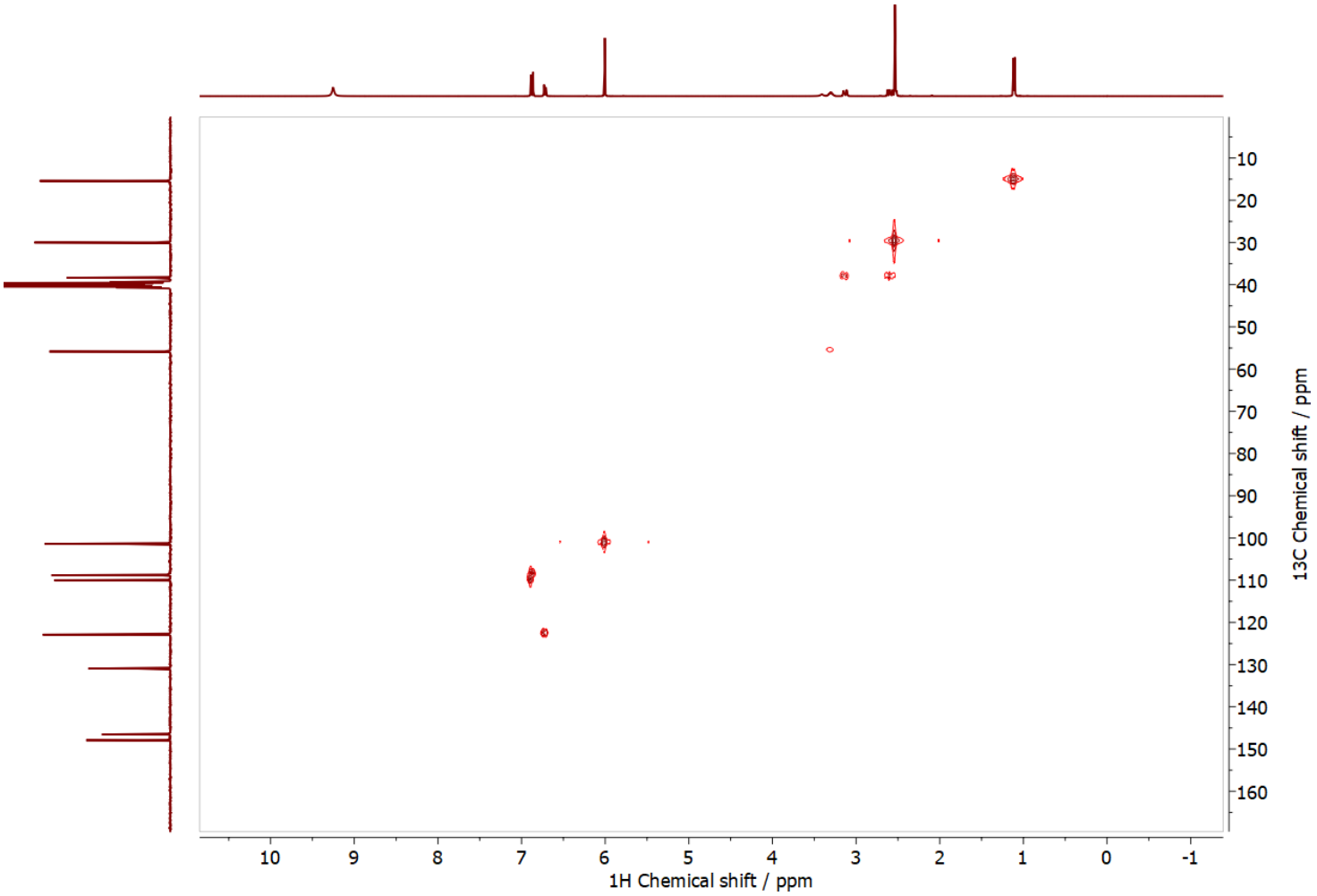


*Figure 12 $^{1}H$-$^{13}C$ HMQC NMR spectrum of MDMA collected in $d_6$-DMSO*

| MDMA | | |
|---|---|---|
| **Position number** | **$^{1}$H NMR δ / ppm** | **$^{13}$C NMR δ / ppm** |
| 1 | 5.99 (2H) | 101.4 |
| 2 | N/A | 147.9 |
| 3 | N/A | 146.5 |
| 4 | 6.87 ($^{4}J_{HH}$ = 1.44 Hz, 1H) | 110.0 |
| 5 | N/A | 130.9 |
| 6 | 6.70 ($^{4}J_{HH}$ = 1.42 Hz and $^{3}J_{HH}$ = 7.88 Hz, 1H) | 122.9 |
| 7 | 6.85 ($^{3}J_{HH}$ = 7.92 Hz, 1H) | 108.8 |
| 8i | 3.11 ($J_{HH}$ = 13.15 Hz and $J_{HH}$ = 4.28 Hz, 1H) | 38.4 |
| 8ii | 2.58 ($J_{HH}$ = 13.15 Hz and $J_{HH}$ = 9.96 Hz, 1H) | 38.4 |
| 9 | 3.25 (1H) | 55.8 |
| 10 | 9.25 (2H) | N/A |
| 11 | 2.52 (3H) | 30.1 |
| 12 | 1.09 ($^{3}J_{HH}$ = 6.52 Hz, 3H) | 15.4 |

*Table 1 Summary of $^{1}$H and $^{13}$C{$^{1}$H} NMR data for MDMA*

### 4.2.2 Gas Chromatography Characterisation

A typical chromatogram for MDMA is provided overleaf (Figure 13). It shows the retention time at which MDMA elutes is at 5.62 minutes and the retention time for eicosane is 7.24 minutes. The chromatogram shows no distortion of the peak shapes, only with very little tailing occurring at base of each peak. The peaks are fairly symmetrical, and the base line shows very little background noise, deeming the method developed and therefore the mass spectrum of MDMA (Figure 14) fit for reliable analysis of the unknown suspected drug samples. Calibration standards were integrated and the peak area ratios (PARs) between MDMA and eicosane were calculated. These were then used to construct calibration series, plotting PAR vs. increasing concentration, producing a linear response.

The limit of detection (LoD) is the lowest concentration of a component that can be reliably detected with a given analytical method. The limit of quantification (LOQ) is lowest concentration at which a component can be reliably measured, once detected, by an analytical method.[68] They can be calculated using the signal to noise ratios (SNR) of the peaks seen in the GC chromatogram. This is simply a comparison of the level of a desired signal to the level of background noise.[69] The LoD and LoQ were calculated as they are more efficient than just using the calibration. They can inform if a method is sensitive enough and can be compared to similar investigations that have already been published. In this instance, they were calculated in order to validate the GC method and was determined using the SNR of LoQ and LoD of 10 + 3.

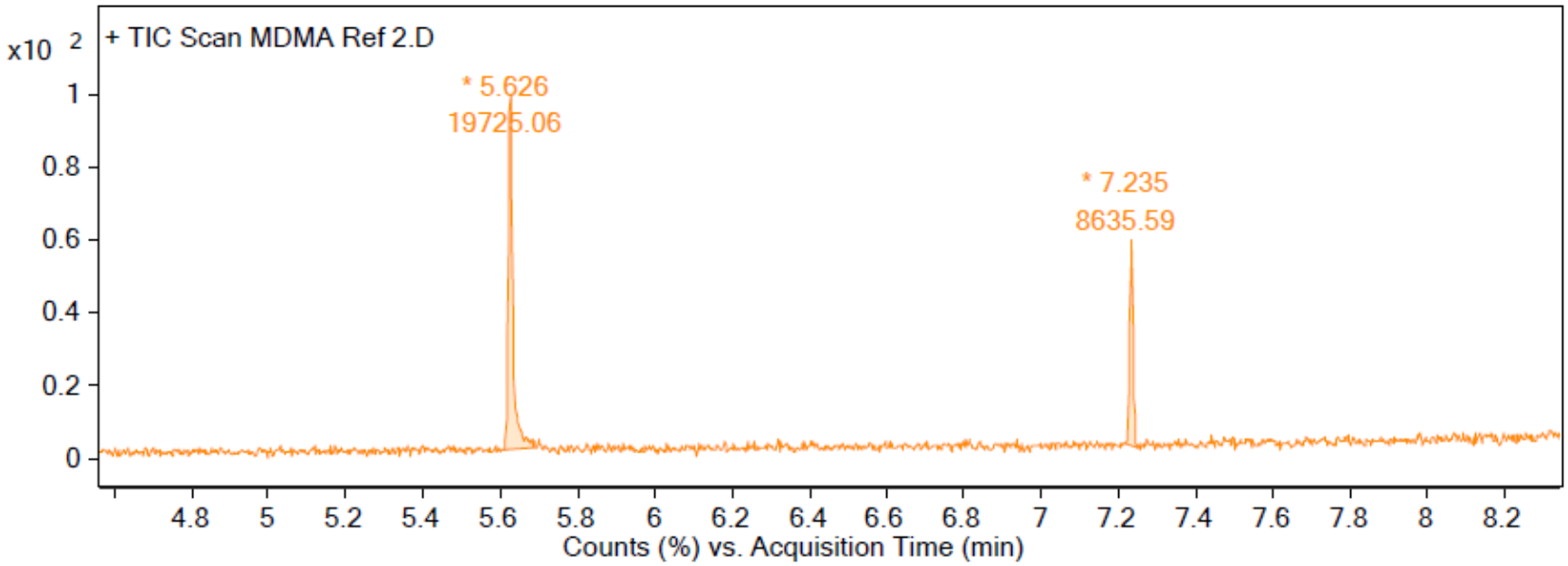


*Figure 13 Gas Chromatogram of MDMA ($R_t$ = 5.626 mins) in a sample spiked with eicosane ($R_t$ = 7.235 mins) collected on an Agilent 6850 GC*

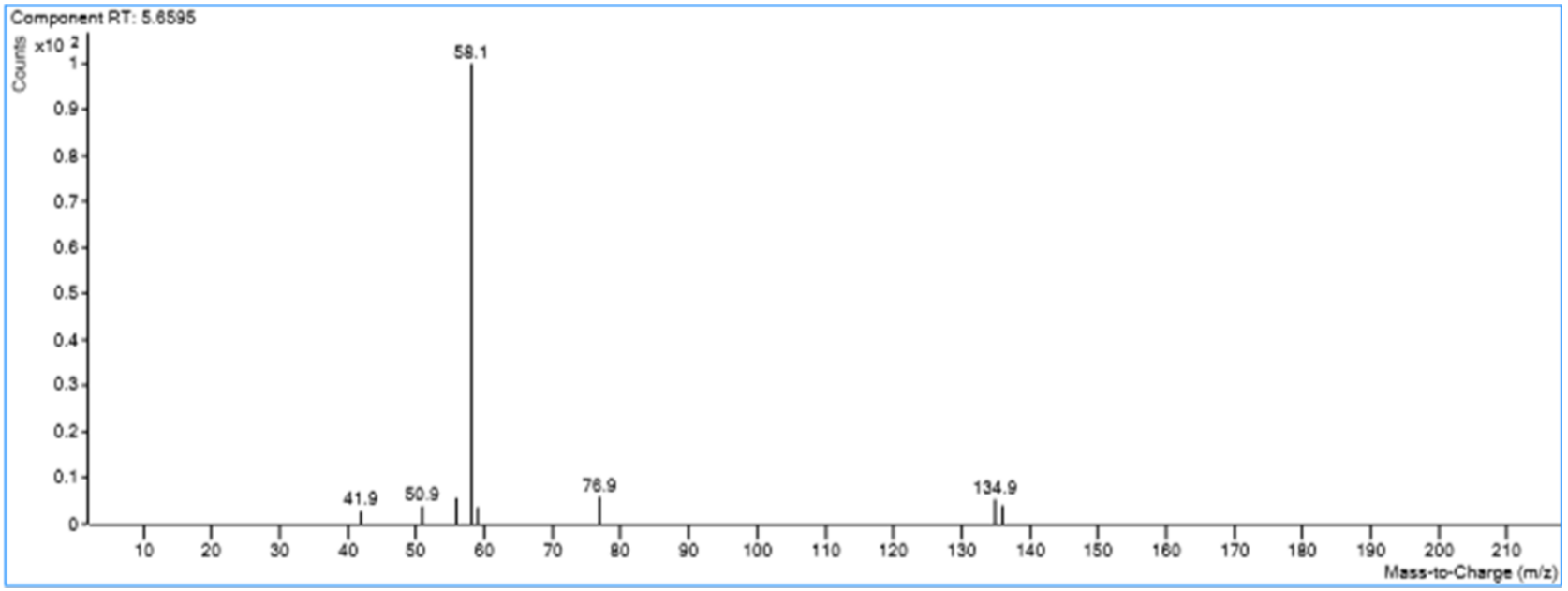


*Figure 14 Mass spectrum of MDMA*

The mass spectrum of MDMA (Figure 14) shows the base peak of the molecule at 58.1 m/z, which is the ion with the greatest relative abundance in the molecule. The peak at 134.9 m/z is the largest fragment shown on the spectrum; however, it is unable to be the molecular ion peak as MDMA has a molecular weight of 193.25 g/mol. This must therefore be the tropylium ion, formed by the fragmentation of an aromatic containing group (Figure 15). The spectrum of MDMA collected on the GC was compared to that available on the Cayman Chemical database[70] (3,4-MDMA (hydrochloride), CAS Number 64057-70-1) and had very close similarity.

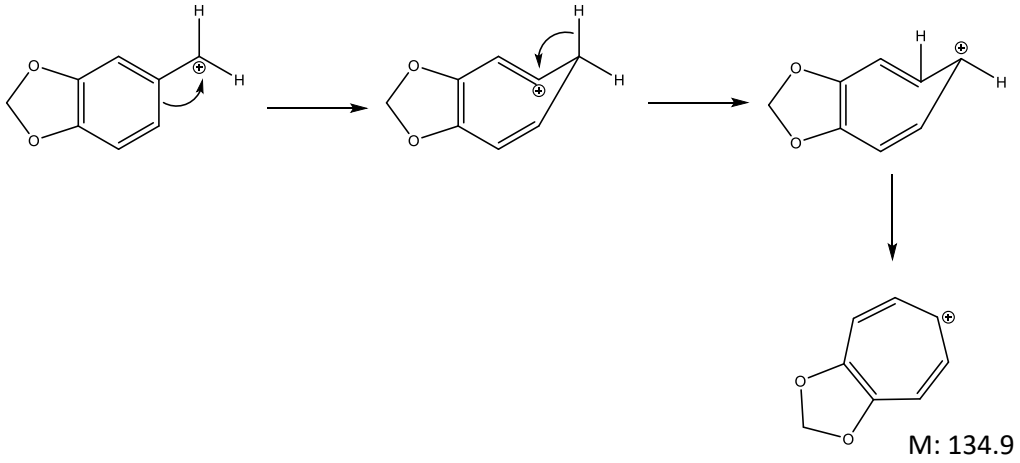


*Figure 15 MDMA tropylium ion formation*

### 4.2.3 Infrared Characterisation

Infrared spectroscopy measures the vibrations of the bonds between the atoms within a molecule and based on this it is possible to determine the functional groups. The structure of MDMA (Figure 7) shows the most prominent functional groups of the molecule to be the aromatic region, the N-H bond and the C-O bond. The infrared spectrum of MDMA (Figure 16) shows the presence of these functional groups at wavenumbers 2946 (N-H), 1488 (aromatic C=C) and at 1032 $cm^{-1}$ (C-O). There are also strong, broad and sharp peaks at 2711 $cm^{-1}$ and 797 $cm^{-1}$ showing the presence of the C-H bonds due to C-H bond stretching taking place.

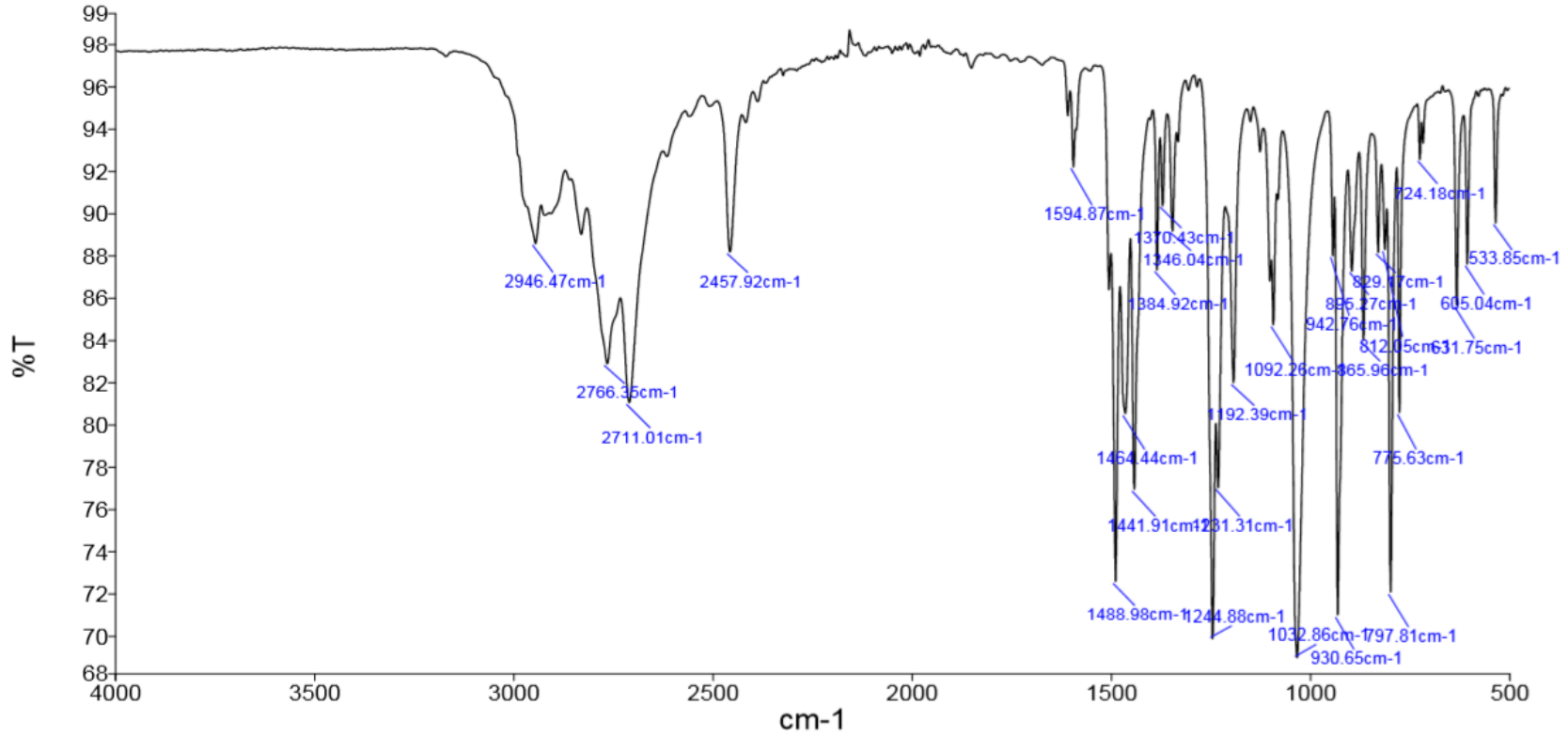


*Figure 16 IR spectrum of MDMA*

## 4.3 PMA Characterisation

MDMA tablets can potentially be adulterated with PMA, so the compound was fully characterised using NMR, GC-MS and IR. The 20 mg/mL $d_6$-DMSO sample was used to carry out the analysis and the structural configuration was determined. This was so it could be identified if found in combination with MDMA.

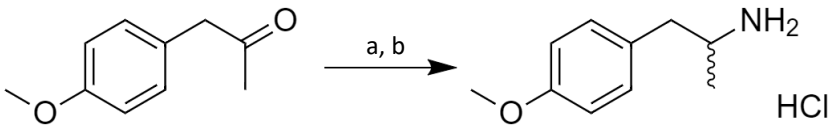


PMA

*Scheme 2 The synthesis of 4-methoxyamphetamine hydrochloride (PMA). Reagents/conditions: (a) $NH_4OAc$ / $NaBH_3CN$ / MeOH / 24h; (b) HCl (4M solution in 1,4-dioxane)*

### 4.3.1 NMR Characterisation

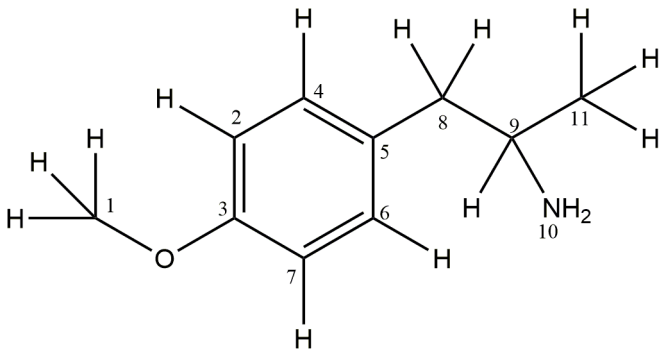


*Figure 17 Chemical structure of PMA with atom labelling shown*

PMA (chemical structure and atom labelling scheme shown in Figure 17) has seven $^1H$ environments and the $^1H$ NMR spectrum shown in Figure 18 reflects this. The protons at positions 2 and 7 occupy the same $^1H$ environment as do the protons at positions 4 and 6. The aliphatic chain of PMA consists of four discrete $^1H$ NMR environments. The signal for the methyl protons at position 11 are observed at 1.05

ppm and integrate to three hydrogens. A $^{3}J_{HH}$ coupling of 8.00 Hz is observed to the chiral centre at position 8. This peak shows a COSY interaction (Figure 19) to a single peak at 3.28 ppm; this peak is the chiral centre located at position 9. The chiral centre (C9) shows coupling to both diastereotopic protons in C8 located at 2.95 and 2.55 ppm. The two diastereotopic protons appear as a doublets of doublets. The signal at 2.94 ppm has two couplings; a $^{2}J_{HH}$ of 13.38 Hz and a $^{3}J_{HH}$ of 4.95 Hz. The other peak at 2.55 ppm has couplings of 13.38 Hz ($^{2}J_{HH}$) and 9.20 Hz ($^{3}J_{HH}$). Due to these two protons being easily interchangeable by rotation, it is difficult to determine exactly which proton corresponds to each peak. The amine protons at position 10 appear as a broad signal at 8.17 ppm in the $^{1}H$ NMR spectrum and integrate to two protons.

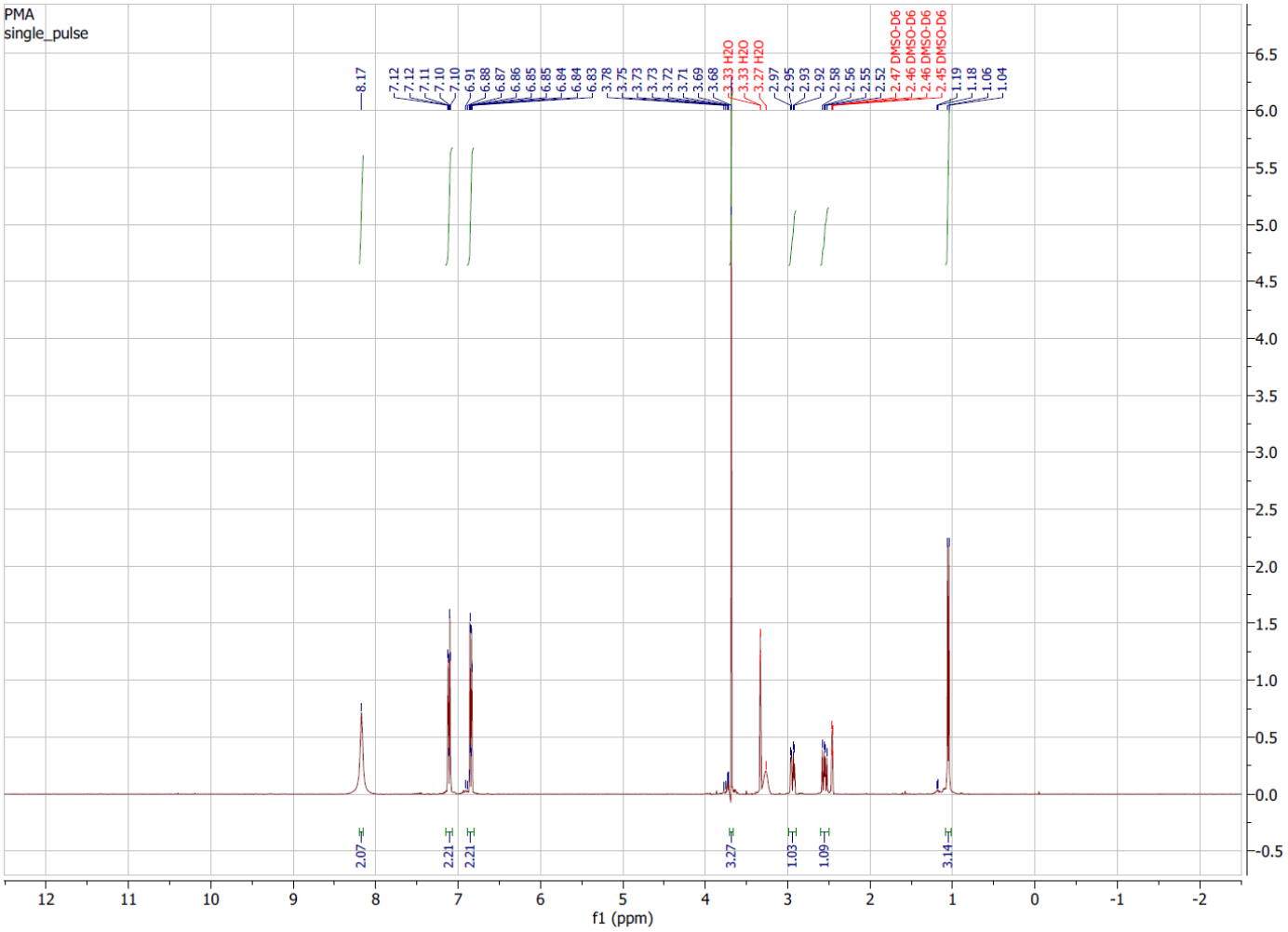


*Figure 18 $^{1}H$ NMR spectrum of PMA collected in $d_6$-DMSO*

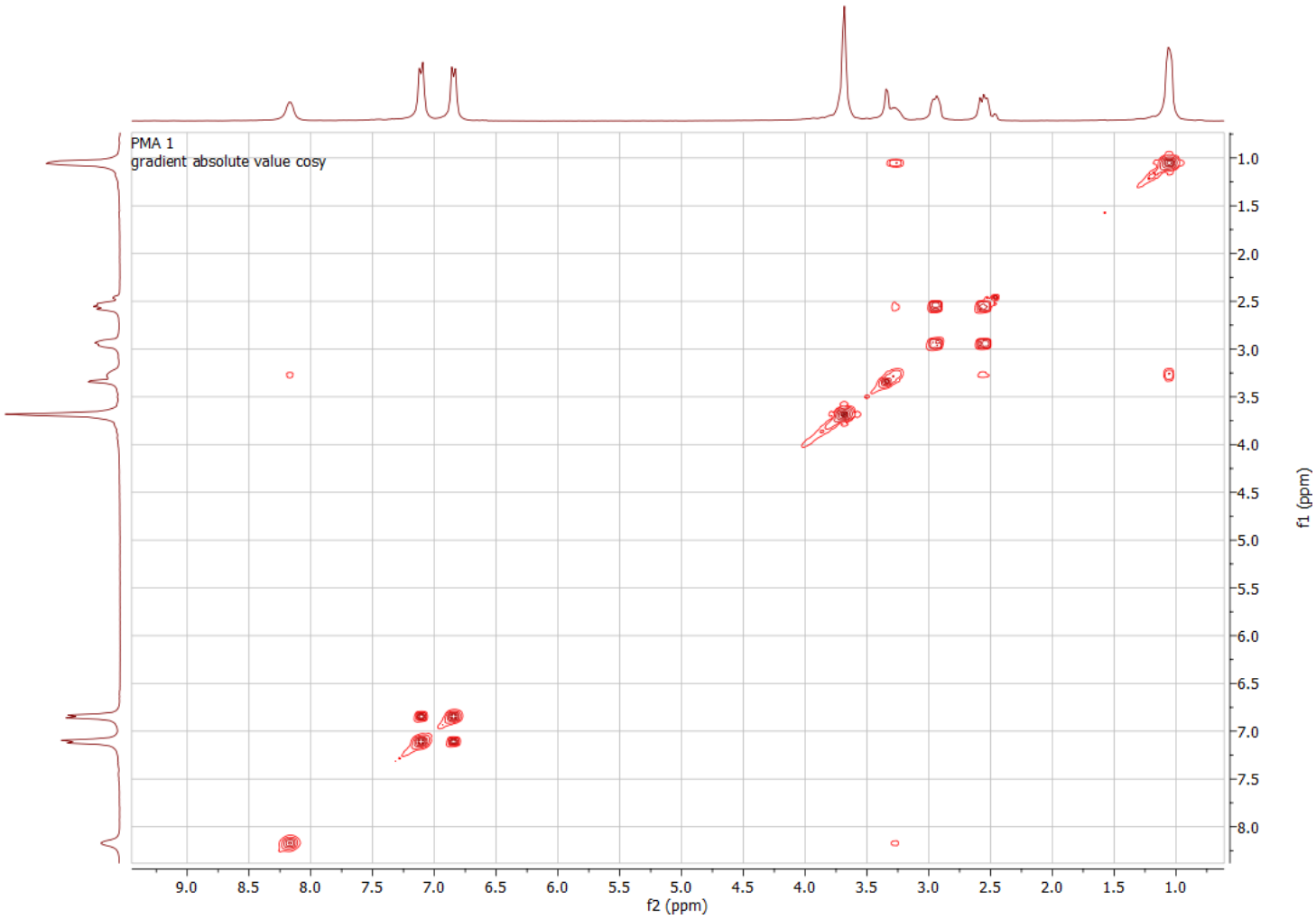


*Figure 19 $^{1}H$-$^{1}H$ COSY NMR spectrum of PMA collected in $d_6$-DMSO*

The aromatic part of the $^{1}H$ NMR spectrum differs significantly to MDMA. This is because of the different substitution patterns of the two molecules; PMA is 1,4-disubstitututed whereas MDMA is 1,3,4-trisubstituted. The four aromatic proton nuclei of PMA are in two discrete environments and are observed at 7.11 and 6.85 ppm on the $^{1}H$ NMR spectrum. They both appear as doublets that display second-order effects. The $^{3}J_{HH}$ coupling for these two environments are 8.42 Hz. As the methoxy group located at position 3 on the aromatic ring (Figure 17) is an electron-donating group and is significantly more electron-donating than the aliphatic chain, this has the effect of shielding the protons *ortho* to it (positions 2 and 7). They are therefore the most shielded, and hence why they appear at 6.85 ppm in the $^{1}H$ NMR spectrum. The protons *meta* to the methoxy group (positions 4 and 6) are only shielded by the aliphatic chain and thus they are more downfield of the other set of aromatic protons – they are present in the $^{1}H$ NMR spectrum at 7.11 ppm. The reciprocal coupling of these two environments is reflected in the $^{1}H$-$^{1}H$ COSY NMR spectrum (Figure 19) by the presence of cross-peaks linking the two environments.

The methoxy protons at position 1 (Figure 17) are isolated in the molecule and show no coupling, as evidenced by the lack of cross-peaks in the $^{1}H$-$^{1}H$ COSY NMR and that these protons present as a singlet in the $^{1}H$ NMR spectrum. They are located at 3.68 ppm; the de-shielded nature of the peak is due to the electron-withdrawing effects of the oxygen.

PMA possesses eight different $^{13}C$ environments and the $^{13}C\{^{1}H\}$ NMR spectrum (Figure 20) reflects this. The aliphatic chain has three different $^{13}C$ environments at positions 8, 9 and 11. The carbon to which the diastereotopic $^{1}H$ nuclei is attached (position 8) is located at 39.7 ppm. This peak is the only $CH_2$ present in PMA and the corresponding DEPT-135 (Figure 21) shows only a single negative peak, which is again observed at 39.7 ppm. Furthermore, the $^{1}H$-$^{13}C$ HMQC NMR spectrum (Figure 22) shows that this peak possesses cross-peaks to both diastereotopic $^{1}H$ nuclei located at 2.94 and 2.55 ppm. In addition, the $^{1}H$-$^{13}C$ HMBC NMR spectrum (Figure 23) shows a cross-peak that links this environment to the aromatic protons ortho to the aliphatic chain located three-bonds away. The methyl carbon of the aliphatic chain at position 11 is located at 17.9 ppm. It is the most shielded carbon environment present in PMA.

The $^{1}H$-$^{13}C$ HMQC NMR spectrum shows a cross peak that links this environment to its corresponding proton nuclei at 1.05 ppm. Lastly, the chiral centre is observed at 48.7 ppm on the $^{13}C$ NMR spectrum. This peak is de-shielded by the adjacent nitrogen atom and is positive in the DEPT-135 NMR spectrum.

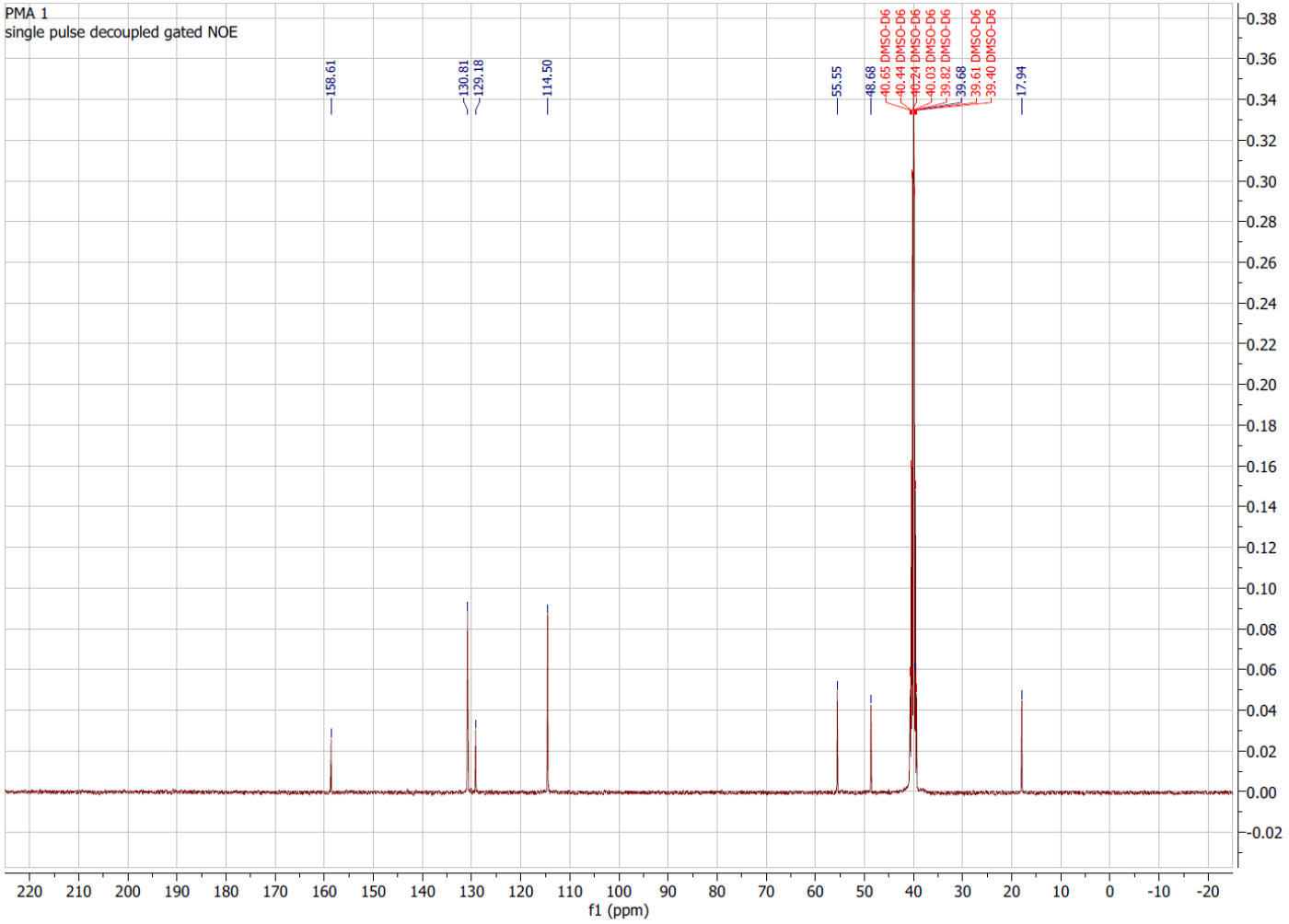


*Figure 20 $^{13}C\{^{1}H\}$ NMR spectrum of PMA collected in $d_6$-DMSO*

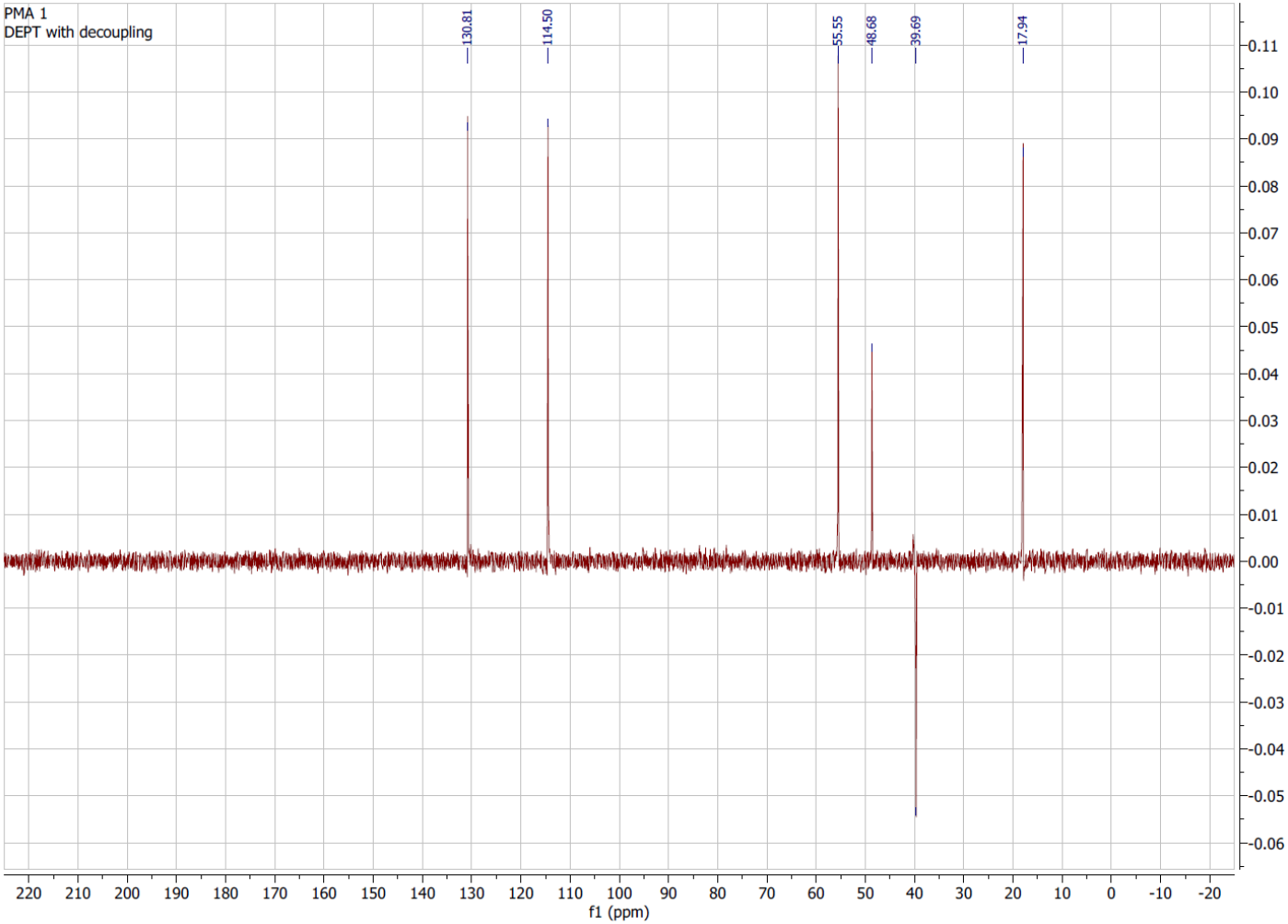


*Figure 21 DEPT-135 $^{13}C\{^{1}H\}$ NMR spectrum of PMA collected in $d_6$-DMSO*

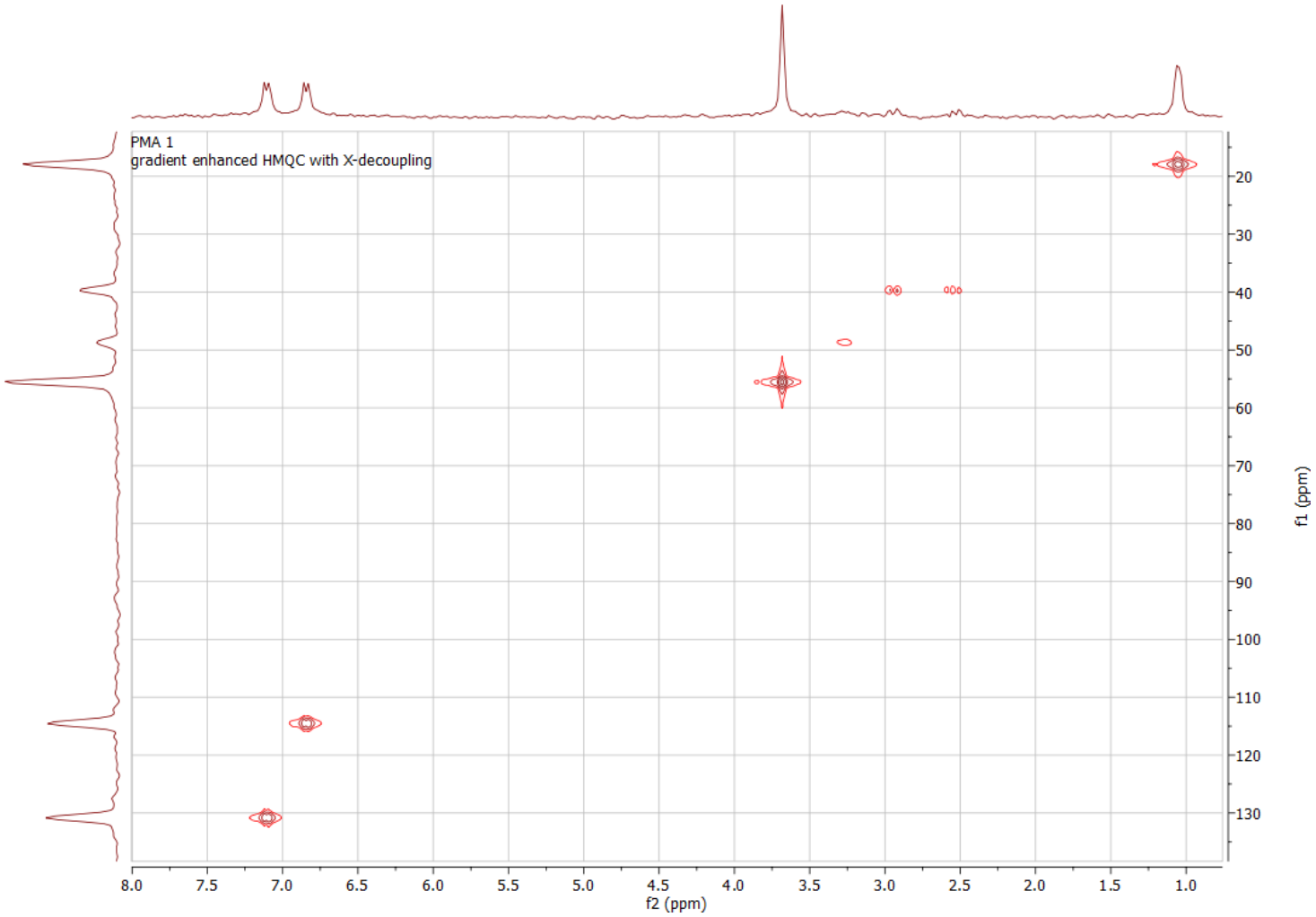


*Figure 22 $^{1}H$-$^{13}C$ HMQC NMR spectrum of PMA collected in $d_6$-DMSO*

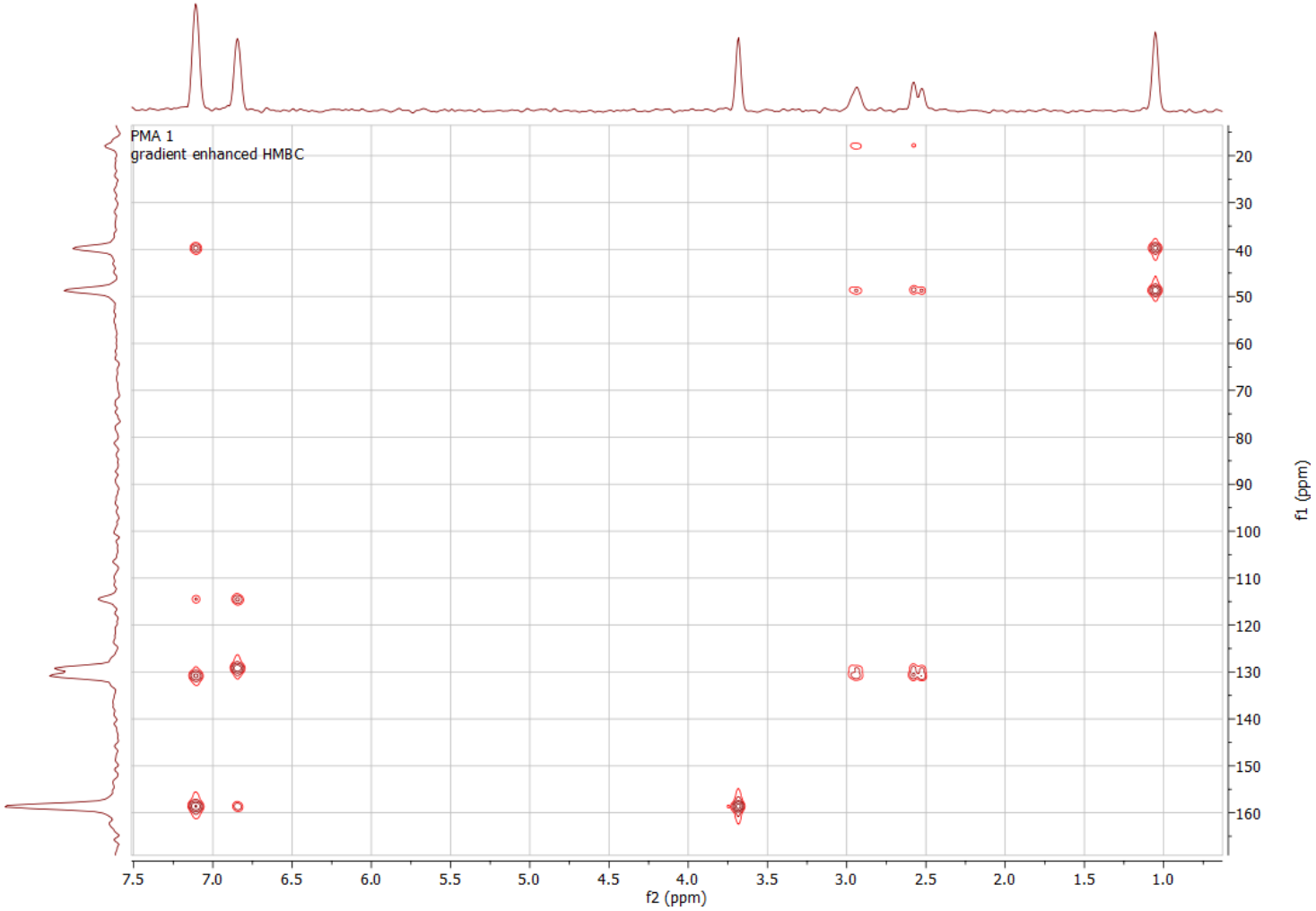


*Figure 23 $^{1}H$-$^{13}C$ HMBC NMR spectrum of PMA collected in $d_6$-DMSO*

There are four aromatic carbons in structure of PMA (Figure 17). Two of these are quaternary and they are located at 158.6 and 129.2 ppm. The former is adjacent to the methoxy group that de-shields the carbon environment whereas the latter is coupled to the $CH_2$ of the aliphatic chain which shields the environment. Both peaks are absent in the DEPT-135 NMR spectrum. Additionally, the peak at 158.6 ppm shows a cross peak to the methoxy protons located three bonds away at 3.26 ppm in the $^{1}H$ NMR spectrum, whereas this interaction is not observed for the other quaternary carbon. The peak at 129.2 ppm instead shows cross-peaks to both diastereotopic protons, which are located two bonds away. Two further peaks are observed at 130.8 and 114.5 ppm. They are both positive in the DEPT-135 NMR spectrum and so are assigned as CH environments. The carbon environments *ortho* to the methoxy group are the most shielded, and hence appear at 114.5 ppm. The other aromatic CH environment is not as shielded and appears at 130.8 ppm.

The methoxy carbon is located at 58.6 ppm in the $^{13}C\{^{1}H\}$ NMR spectrum. This peak is significantly more deshielded than the chiral centre. This peak shows a cross-peak to its corresponding proton nuclei located at 3.68 ppm in the $^{1}H$ NMR spectrum.

| PMA | | |
|---|---|---|
| **Position number** | **$^{1}$H NMR δ / ppm** | **$^{13}$C NMR δ / ppm** |
| 1 | 3.68 (3H) | 55.6 |
| 2 | 6.85 ($^{3}J_{HH}$ 8.42 Hz, 1H) | 114.5 |
| 3 | N/A | 158.6 |
| 4 | 7.11 ($^{3}J_{HH}$ 8.42 Hz, 1H) | 130.8 |
| 5 | N/A | 129.2 |
| 6 | 7.11 ($^{3}J_{HH}$ 8.42 Hz, 1H) | 130.8 |
| 7 | 6.85 ($^{3}J_{HH}$ 8.42 Hz, 1H) | 114.5 |
| 8i | 2.94 ($^{2}J_{HH}$ = 13.38 Hz and $^{3}J_{HH}$ = 4.95 Hz, 1H) | 39.7 |
| 8ii | 2.55 ($^{2}J_{HH}$ = 13.38 Hz and $^{3}J_{HH}$ = 9.20 Hz, 1H) | 39.7 |
| 9 | 3.26 (1H) | 48.7 |
| 10 | 8.17 (2H) | N/A |
| 11 | 1.05 ($^{3}J_{HH}$ = 8.00 Hz, 3H) | 17.9 |

*Table 2 Summary of $^{1}$H and $^{13}$C NMR data for PMA*

### 4.3.2 Gas Chromatography Characterisation

The chemical structure of PMA is similar to that of MDMA, however they have significantly different sized base peaks and PMA is structurally smaller than MDMA. This would suggest both compounds would elute at different retention times, and looking at the chromatograms of each drug, it is seen that MDMA (Figure 13) and PMA (Figure 25) would elute at 5.62 and 4.96 minutes respectively. This suggests that if a sample was to appear consisting of both these structures, the GC could successfully elucidate that both components were present.

The mass spectrum of PMA (Figure 26) shows the base peak of the molecule at 44.0 m/z, which is the ion with the greatest relative abundance in the molecule. The peak at 122 m/z is the largest fragment shown on the spectrum; however, it is unable to be the molecular ion peak as PMA has a molecular weight of 165.23 g/mol. This must therefore be the tropylium ion (Figure 24). The spectrum of PMA collected on the GC was compared to that available on the Cayman Chemical database[71] (4-methoxyamphetamine (hydrochloride), CAS Number 3706-26-1) and had very close similarity.

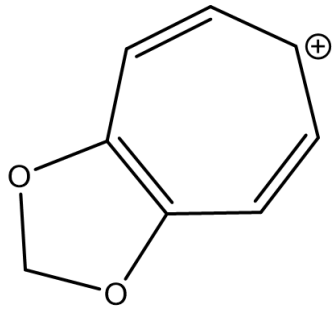


*Figure 24 Tropylium ion*

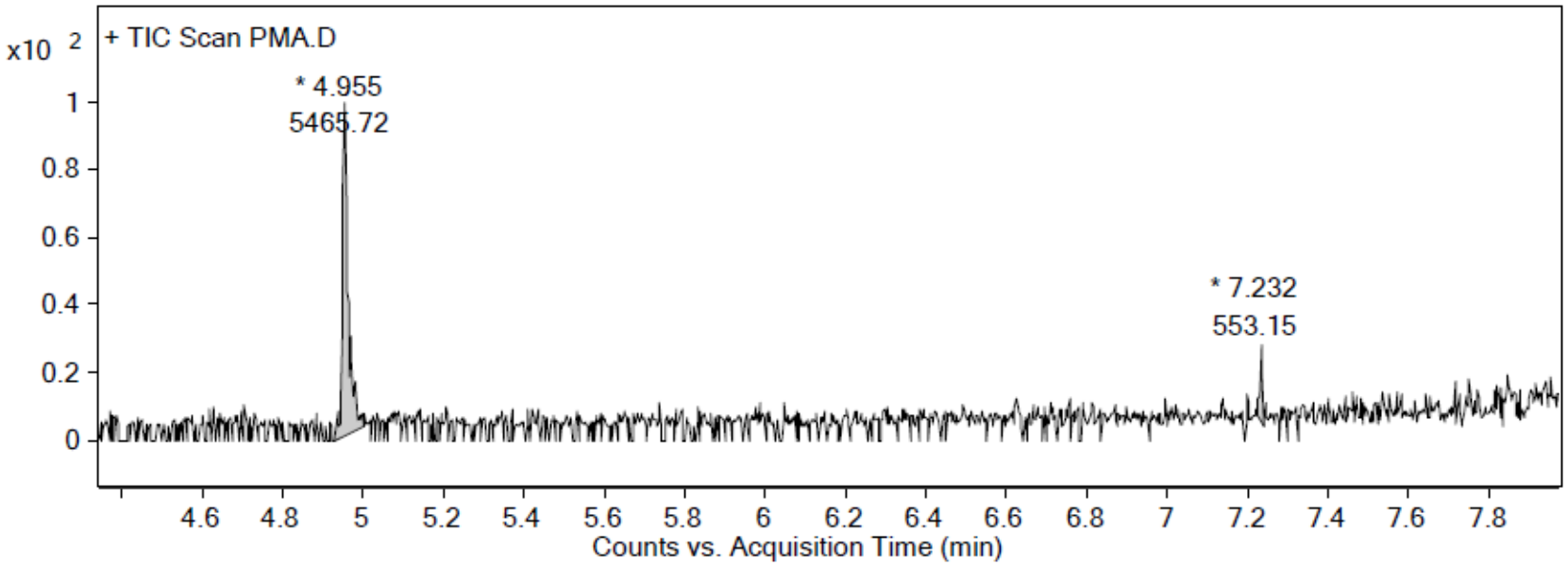


*Figure 25 Gas Chromatogram of PMA collected on an Agilent 6850 GC*

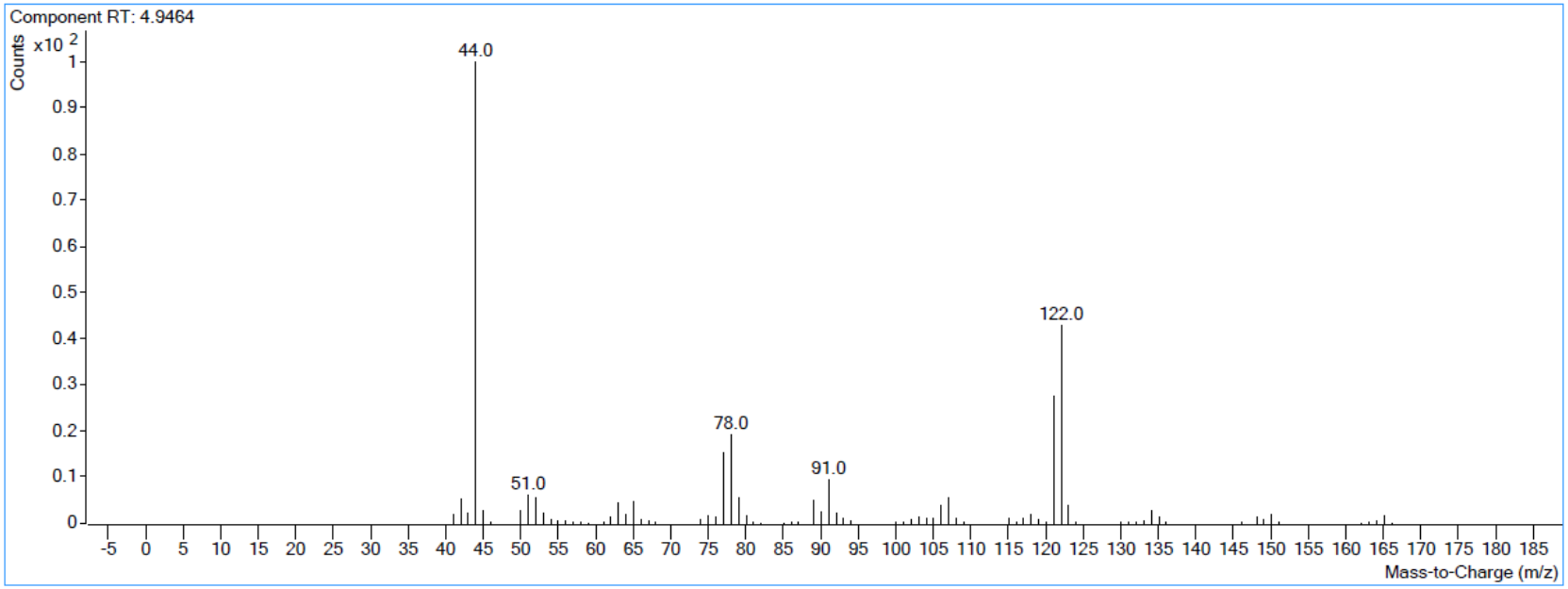


*Figure 26 Mass spectrum of PMA*

### 4.3.3 Infrared Characterisation

The chemical structure of PMA (Figure 17) shows the most prominent functional groups of the molecule to be the aromatic region, the N-H bond and the C-O bond. The infrared spectrum of PMA (Figure 27) shows the presence of these functional groups at 2913 (N-H), 1507 (aromatic C=C) and at 1031 $cm^{-1}$ (O-$CH_3$). There is also a strong, sharp peak at 807 $cm^{-1}$ showing the presence of the C-H bonds due to C-H stretching.

In comparison to the IR spectrum of MDMA, the spectrum of PMA looks visually similar. As PMA and MDMA possess the same functional groups, and thus have similar stretches in the IR spectrum, it would be virtually impossible to identify both drugs being present in a mixture just using infrared spectroscopy with any degree of certainty. Therefore, IR data should be used in combination with other analytical techniques, such as NMR and GC-MS, when analysing samples suspected of consisting of both MDMA and PMA.

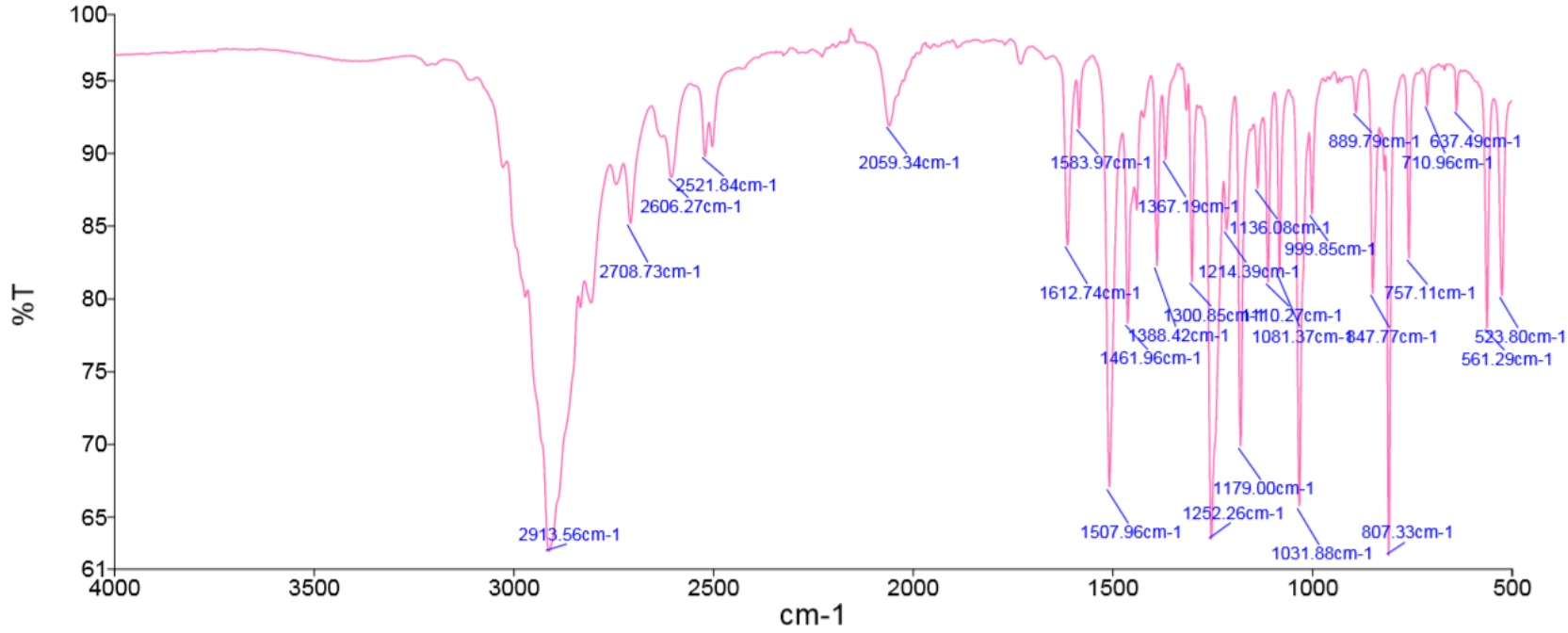


*Figure 27 IR spectrum of PMA*

## 4.4 Qualitative NMR results

Prior to quantifying the amount of PMA and MDMA present in a sample, the samples were qualitatively analysed. 25 samples were provided by GMP for this purpose. Qualitatively analysis was performed on a 60 MHz $^{1}$H NMR spectrometer using an automated process as outlined in section 3. The pattern recognition algorithm employs a minimum distance classifier. The multivariate distance between the sample spectrum and each of the reference spectra is calculated. The sample is identified as the nearest reference compound, provided the 'match score' (equal to one minus the distance of the peaks to the reference spectra), exceeds an empirically determined threshold; if it does not, then the outcome is tentative, unreliable or unknown. The samples analysed were all identified as MDMA with hit scores of greater than 92.3%.

The suspected drug samples were labelled with reference to their appearance. For example, the seized pink bear drug samples shown in Figure 6 were labelled 'PB' and numbered accordingly. So, the $^{1}$H NMR spectrum labelled PB02-04 would show the fourth $^{1}$H NMR scan for the second pink bear tablet. A large quantity of the tablet's supplied were almost equivalent in size, weight and appearance: for example, the pink bear tablets all contained MDMA when qualitatively analysed using $^{1}$H NMR spectroscopy. Therefore, it was assumed these drugs were manufactured simultaneously and came from the same batch. The $^{1}$H NMR spectra for all the PB tablet samples were stacked (Figure 28) and showed they were indeed identical in appearance. They also contained the identifiable MDMA peaks present in the $^{1}$H NMR spectra: benzene, $CH_2$ and methyl, confirming the samples contained MDMA. This would suggest that the batch-to-batch variability of this batch of MDMA tablets to be fairly low and had good uniformity. However, qualitative analysis using the NMR calibration graphs and the integrated NMR spectra for these samples showed all tablets had slightly different concentrations of MDMA per tablet, varying from 190.2 to 228.5 mg MDMA per tablet. This therefore proved the batch to batch variability of the tablets to be higher than first suspected.

The remaining tablet samples were grouped separately as they shared no similarities in appearance. The $^{1}H$ NMR spectra for the samples were stacked (Figure 29) and showed similarities in appearance. They all contained the MDMA peaks present in the $^{1}H$ NMR spectra, confirming the samples contained MDMA. Using the NMR calibration graphs and the integrated NMR spectra for these samples, qualitative analysis of this batch gave results within the range stated by the EMCDDA and gave reasonable figures to be compared to the gold standard GC method.

As the qualitative analysis of the seized samples revealed that only MDMA was present, quantification methods were developed solely for MDMA. NMR and GC-MS were selected as the techniques to be used to quantify MDMA. Firstly, an NMR method was developed, that began with a consideration of the $T_1$ values of specific resonances of MDMA.

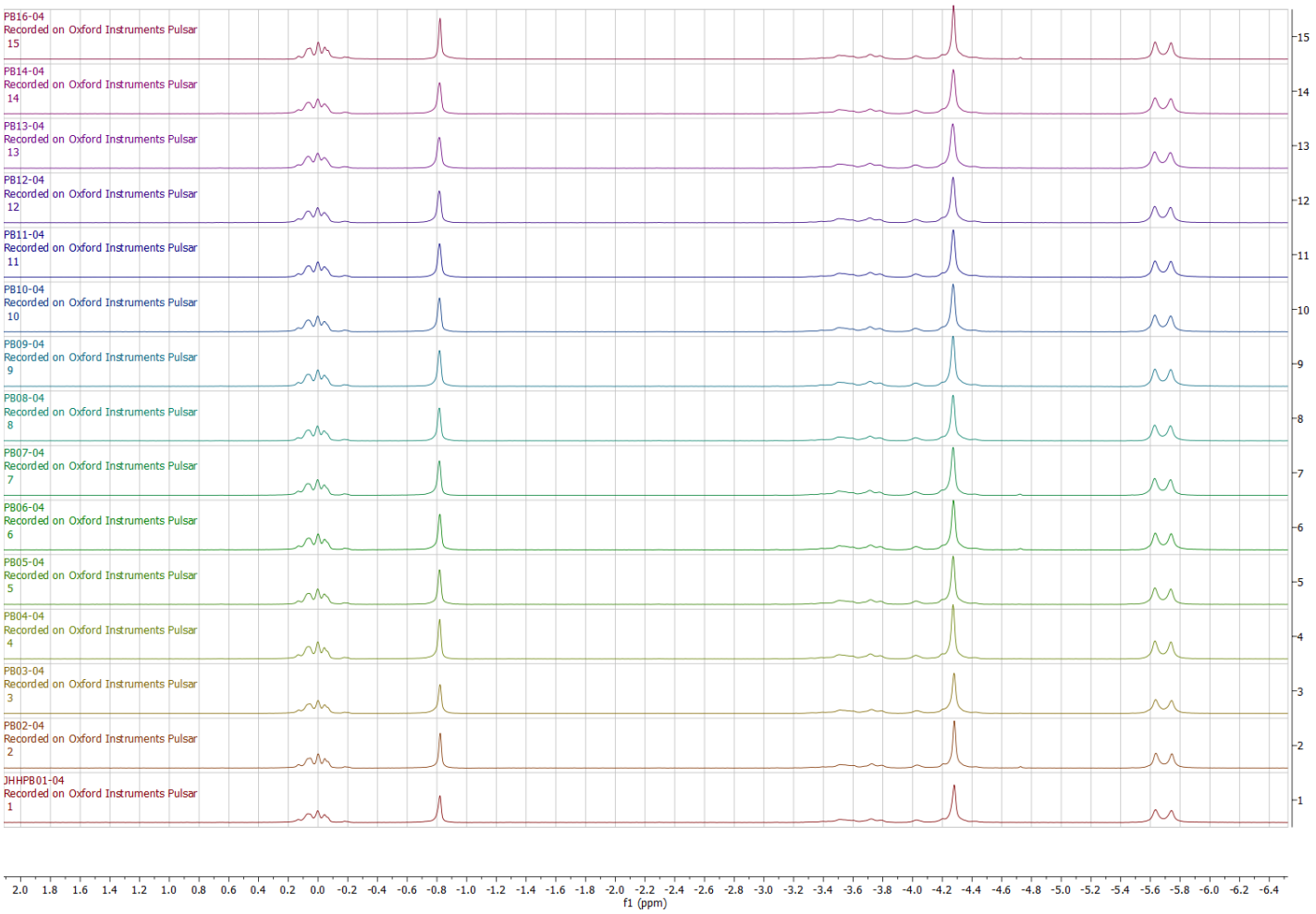


*Figure 28 $^{1}H$ NMR spectra of pink bear tablets which were confirmed to contain MDMA*

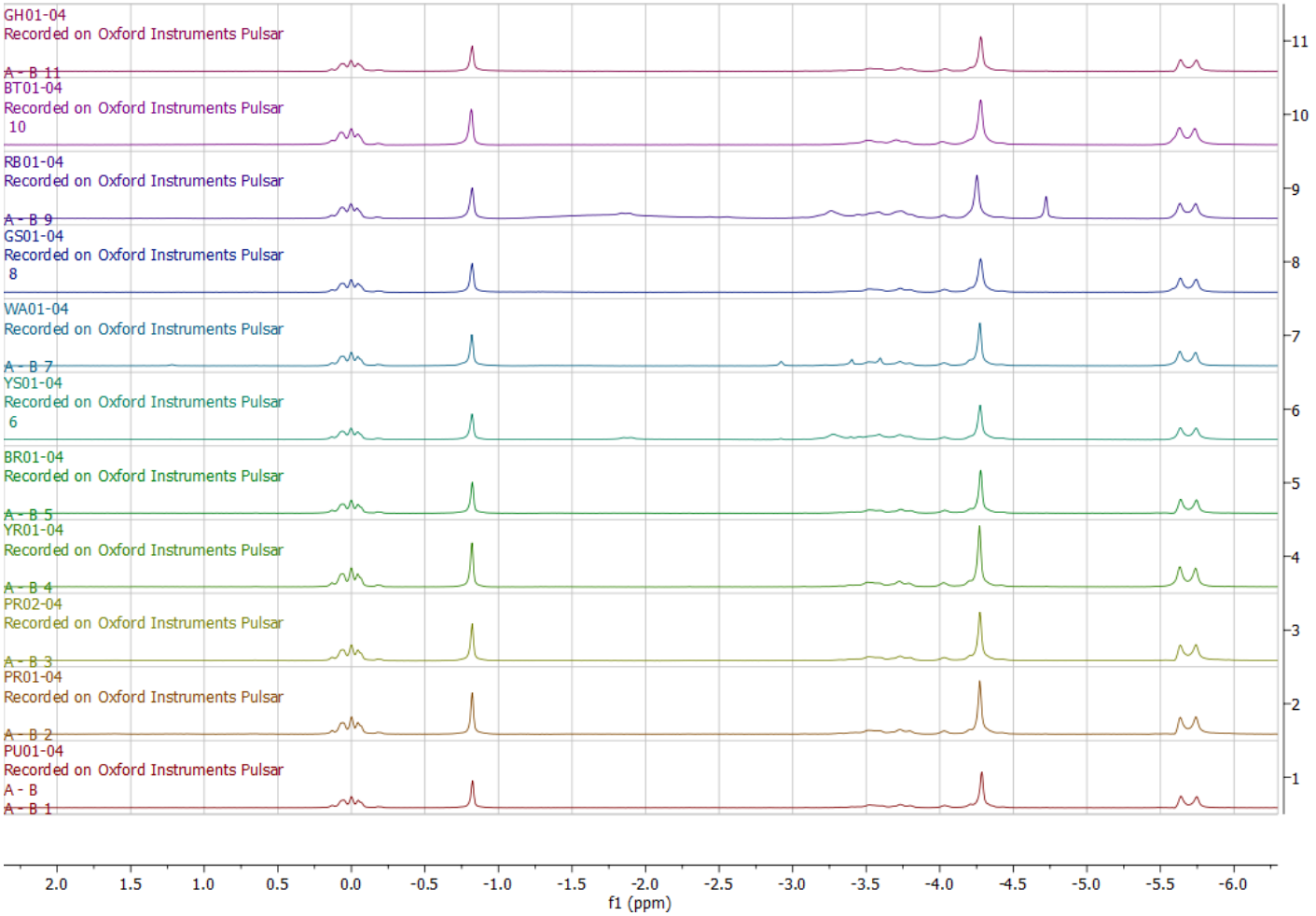


*Figure 29 $^{1}H$ NMR spectra of a range of tablets which were confirmed to contain MDMA*

## 4.5 Quantification of MDMA by NMR

### 4.5.1 $T_1$ data for MDMA

The $T_1$ relaxation time, also known as the spin-lattice (or longitudinal) relaxation time, is used in NMR to quantify the rate of transfer of energy from the nuclear spin system to its neighbouring molecules,[72] i.e. it is a measure of how quickly the nuclear spin recovers to its ground state in the direction of the z-axis. The return of excited nuclei from the high energy state to the low energy or ground state is associated with loss of energy to the surrounding nuclei. The $T_1$ relaxation rate is the reciprocal of the time ($1/T_1$)[73] and is simply another way to express the relaxation time. $T_1$ relaxation is fastest when the rotation of the nucleus, from its ground state to an excited state, matches that of the Larmor frequency. The Larmor frequency refers to the rate of change in the orientation of the rotational axis of the magnetic moment of the proton around the external magnetic field.[74] As a result, $T_1$ relaxation is dependent on the main magnetic field strength. Molecules with stronger bonds will have a higher magnetic field strength and will ultimately be associated with longer $T_1$ times. As the concentration of the sample increases, the $T_1$ is expected to decrease. As the concentration of the sample increases, the $T_1$ is expected to decrease. The shorter the $T_1$, the quicker the return of excited nuclei from the high energy state to its ground state.

$T_1$ plots were produced for 5, 50, 75, 100, 125, 150, 200, 250 and 300 mg/mL MDMA in $d_6$-DMSO samples and the aromatic (Ar), $CH_2$ and Me environments were integrated. The results were tabulated (Table 3) and a calibration graph was produced (Figure 30). The graph supports the definition of how the $T_1$ is expecting to change as concentration changes as it clearly demonstrates a negative gradient showing that the $T_1$ decreases for each concentration at each environment as the concentration of the sample increases.

| | $T_1$ (s) | | |
|---|---|---|---|
| **MDMA conc. (mg/mL)** | **Aromatics** | **$CH_2$** | **$CH_3$** |
| 5 | 1.79 | 1.24 | 0.55 |
| 50 | 1.45 | 1.03 | 0.48 |
| 75 | 1.36 | 0.91 | 0.46 |
| 100 | 1.3 | 0.83 | 0.43 |
| 125 | 1.14 | 0.73 | 0.4 |
| 150 | 1.08 | 0.69 | 0.38 |
| 200 | 0.93 | 0.62 | 0.36 |
| 250 | 0.82 | 0.52 | 0.32 |
| 300 | 0.72 | 0.47 | 0.28 |

*Table 3 Change in $T_1$ with varying concentrations of MDMA (mg/mL)*

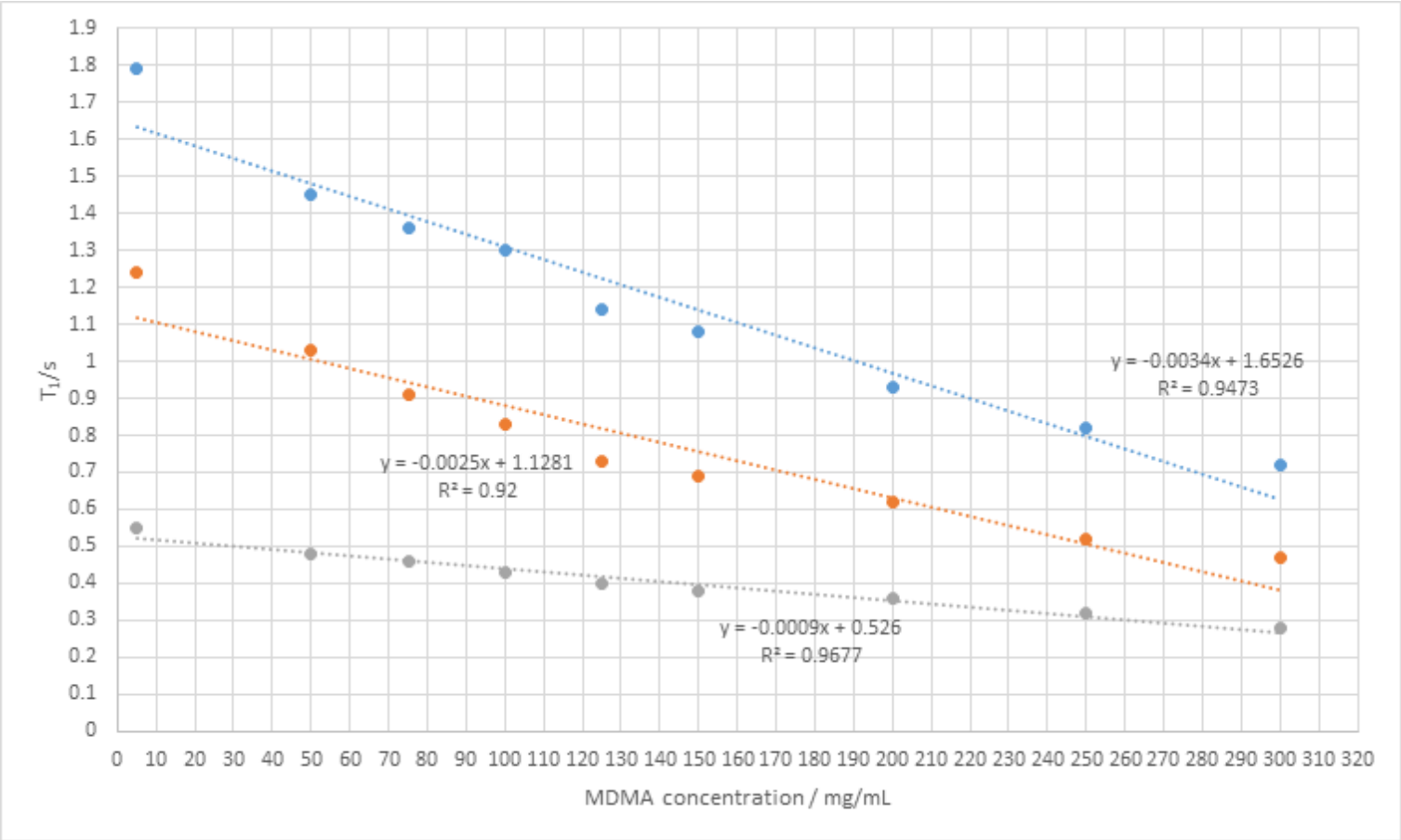


*Figure 30 Change in $T_1$ with varying concentrations of MDMA (mg/mL)*

### 4.5.2 NMR Calibration

A calibration curve was produced using known concentrations of MDMA in order to determine the concentration of MDMA present if found in suspected drug samples. The precision and accuracy of the concentration calculated for the unknowns using the graph are dependent on the calibration curve, specifically the $R^2$ value, which describes the linearity of the graph and how close the data points are to the fitted line of regression.

The MDMA in $d_6$-DMSO standards were analysed using $^1H$ NMR and the results tabulated (Table 4). These data were used to produce 3 calibration curves using the three most prominent peaks visible in the $^1H$ NMR spectrum: the phenyl ring (Figure 31), the dioxymethylene $CH_2$ (Figure 32) and the methyl adjacent to the chiral centre (Figure 33). These environments were chosen as they were isolated, therefore more accessible and easier to pick out. The $^1H$ spectrum of MDMA (Figure 8) proves this as the environments do not interact with each other or any other proton environments in the molecular structure. The amounts of MDMA chosen were 50 - 300 mg/mL MDMA in $d_6$-DMSO as the EMCDDA shows people undertaking in drug festival analysis shows a range of concentrations for the substance so the dose of 300 mg/mL was chosen to encompass all potential doses that have perceived to be circulating.

The graphs had good linearity with an $R^2$ value of 0.9979, so therefore using the calibration graphs, the quality of the calibration standards was able to be assessed and the gradient of the graph would ultimately be used to determine the concentration of MDMA in a sample by comparing the unknown to a set of standard samples of known concentration.

| MDMA conc. (mg/mL) | Integral i (Ar) | Integral ii ($CH_2$) | Integral iii (Me) | Ar conc. (mg/mL) | $CH_2$ conc. (mg/mL) | Me conc. (mg/mL) |
|---|---|---|---|---|---|---|
| 50 | 1 | 1 | 1 | 45.40 | 42.76 | 43.31 |
| 100 | 1.83 | 1.84 | 1.89 | 99.30 | 99.91 | 102.25 |
| 150 | 2.69 | 2.7 | 2.78 | 155.14 | 158.41 | 161.19 |
| 200 | 3.44 | 3.4 | 3.3 | 203.85 | 206.03 | 195.62 |
| 250 | 4.15 | 4.08 | 4.13 | 249.95 | 252.29 | 250.59 |
| 300 | 4.84 | 4.67 | 4.84 | 294.75 | 292.42 | 297.61 |

*Table 4 Calibration table for the aromatic, $CH_2$ and methyl $^1H$ nuclei of MDMA over the range 50 -300 mg/mL and concentrations calculated using calibration plots*

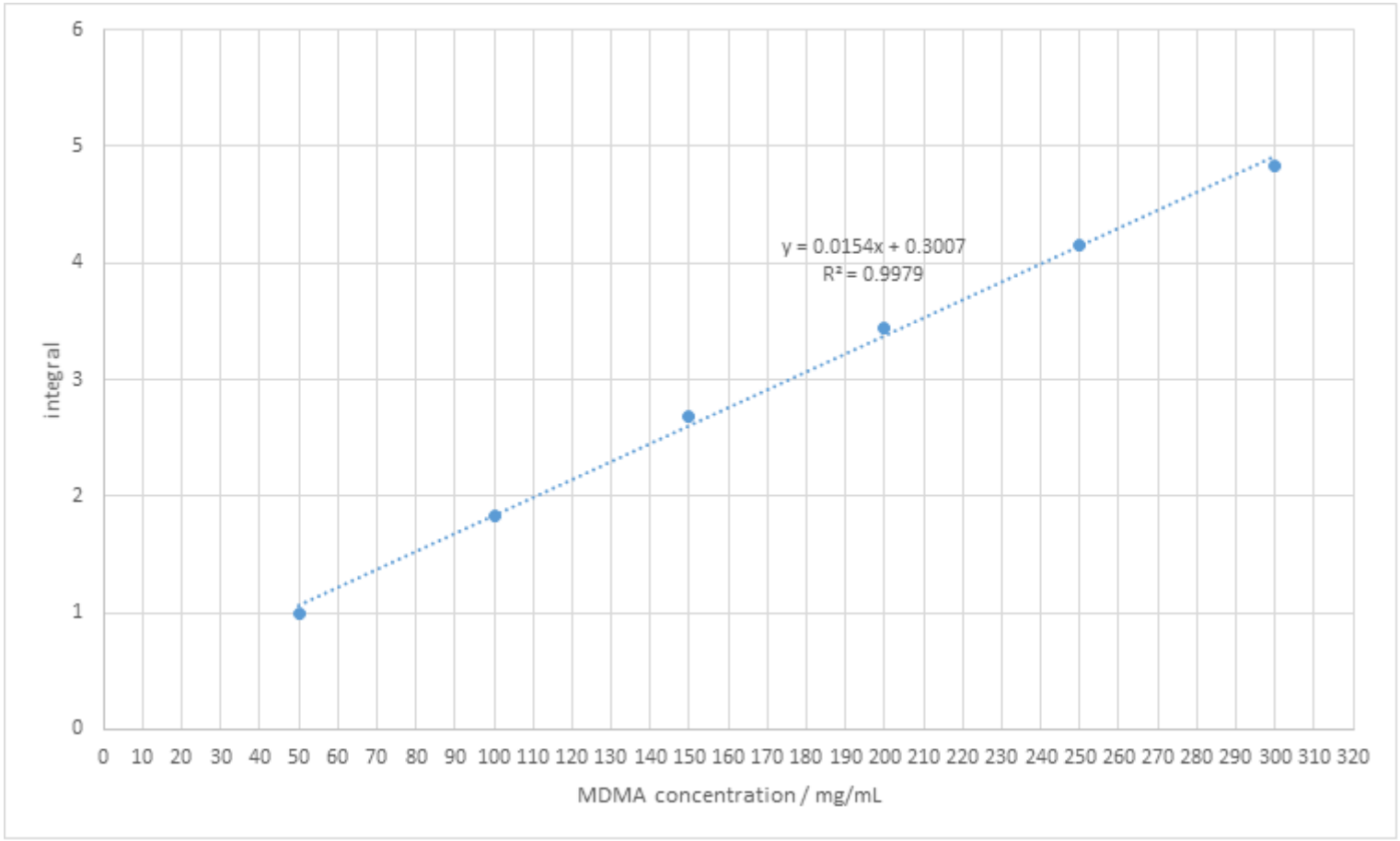


*Figure 31: Calibration plot for the aromatic $^{1}H$ nuclei of MDMA over the range 50 -300 mg/mL. The abscissa provides the normalised integral for each concentration analysed*

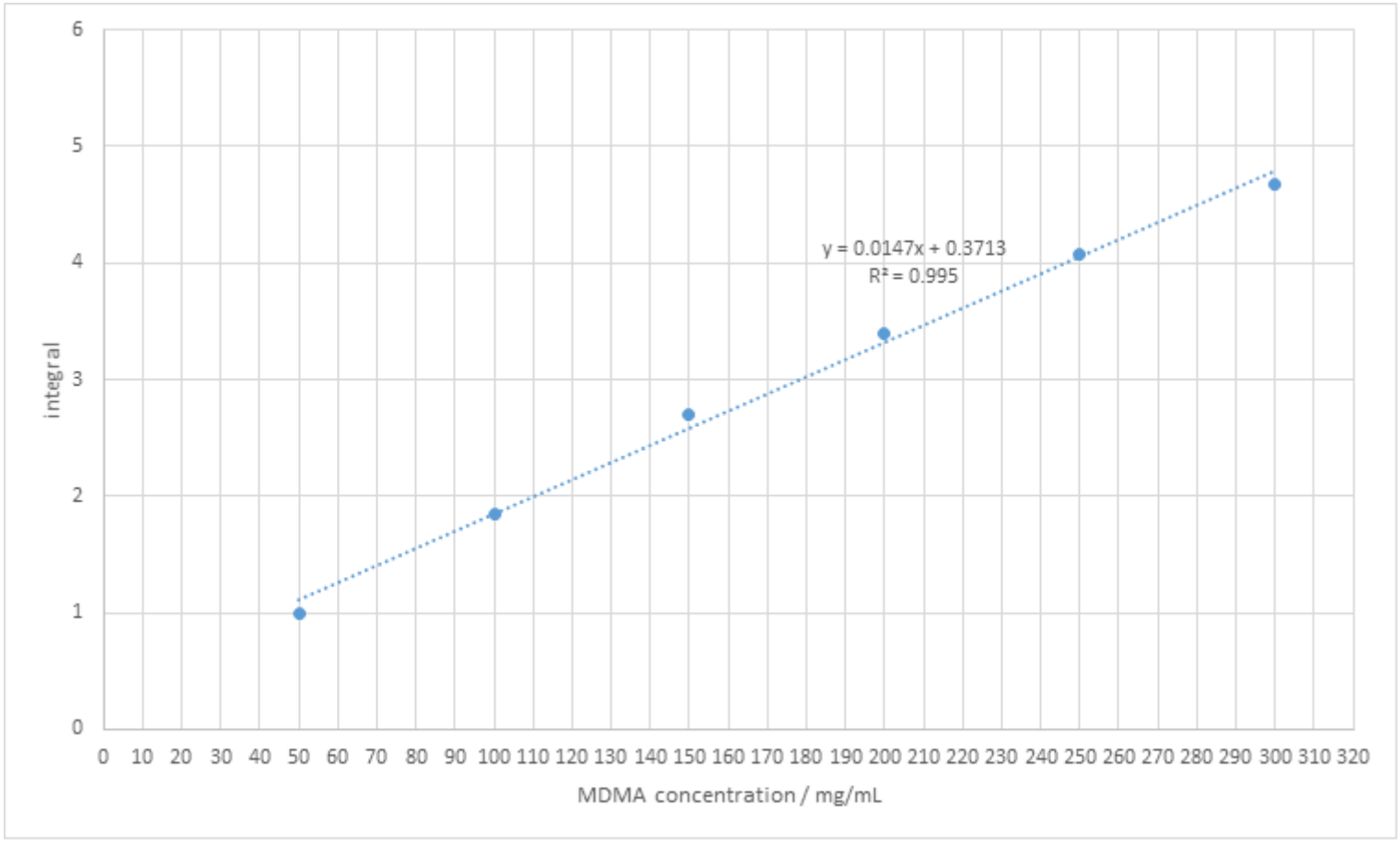


*Figure 32 Calibration plot for the $CH_2$ $^1H$ nuclei of MDMA over the range 50 -300 mg/mL. The abscissa provides the normalised integral for each concentration analysed*

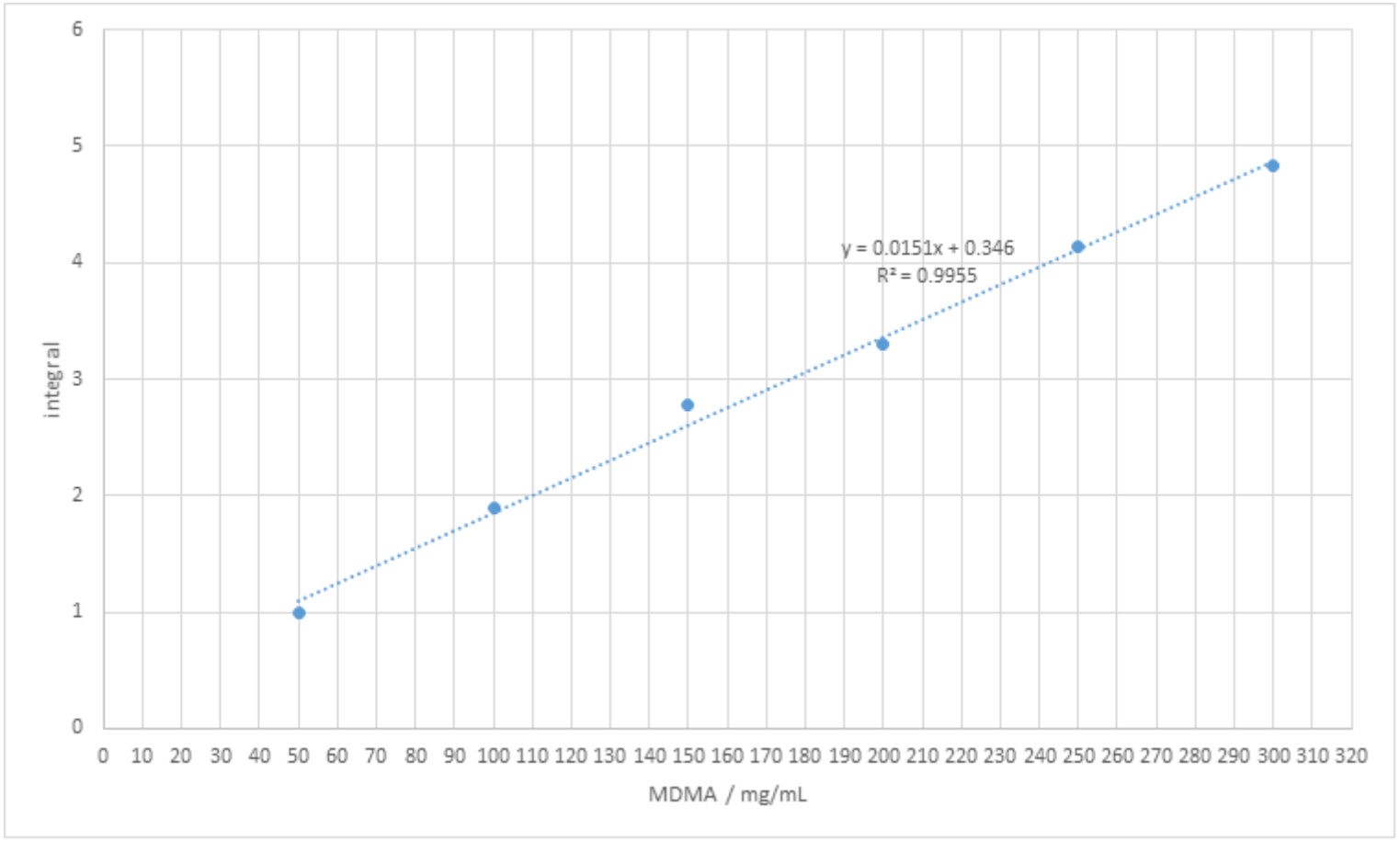


*Figure 33 Calibration plot for the methyl $^{1}H$ nuclei of MDMA over the range 50 -300 mg/mL. The abscissa provides the normalised integral for each concentration analysed*

### 4.5.3 Errors associated with the NMR quantification method

Errors were calculated for the results of the MDMA NMR calibration (Table 5) using the calibration graphs and, due to all the values being known, the precision of the calculations were able to be determined. The $R^2$ value is statistical measure of how close the data are to the line of best fit, and the closer to 1 the value is, the better correlation there is between the two variables in question. In this case the plots showed good linearity, with $R^2$ values of over 0.9950. Removal of each of the points allows to calculate errors associated with this plot, this was then tabulated and shows that the average error on each of the points was approximately 2.36%, which equates to 4.13 mg of MDMA. The result is given as a percentage relative standard deviation (%RSD), which is a measure of precision and of how repeatable the method is. This is calculated using the equation:

$$\%\mathrm{RSD} = \left(\frac{\mathrm{SD}}{\mathrm{mean}}\right) \times 100$$

where SD = the standard deviation and the mean = the mean of all the values.

In order for the experiment to have good repeatability, the %RSD must be no greater that 2%, this means if somebody else was to repeat the experiment exactly, they should get exactly same result less than 2% within error range. The %RSD calculated for the calibration graphs is approximately 2% which shows that method is reproducible.

| Conc. all points included / mg/mL | | | Conc. removed point 1 / mg/mL | | | Conc. removed point 2/ mg/mL | | |
|---|---|---|---|---|---|---|---|---|
| **Ar** | **$CH_2$** | **Me** | **Ar** | **$CH_2$** | **Me** | **Ar** | **$CH_2$** | **Me** |
| 45.40 | 42.76 | 43.31 | 40.13 | 33.90 | 35.31 | 45.05 | 42.59 | 44.46 |
| 99.30 | 99.91 | 102.25 | 95.46 | 93.47 | 96.68 | 98.94 | 99.73 | 103.01 |
| 155.14 | 158.41 | 161.19 | 152.80 | 154.46 | 158.06 | 154.79 | 158.23 | 161.57 |
| 203.85 | 206.03 | 195.62 | 202.80 | 204.11 | 193.93 | 203.49 | 205.85 | 195.78 |
| 249.95 | 252.29 | 250.59 | 250.13 | 252.34 | 251.17 | 249.59 | 252.11 | 250.38 |
| 294.75 | 292.42 | 297.61 | 296.13 | 294.18 | 300.13 | 294.40 | 292.25 | 297.09 |

| Conc. removed point 3/ mg/mL | | | Conc. removed point 4/ mg/mL | | | Conc. removed point 5/ mg/mL | | |
|---|---|---|---|---|---|---|---|---|
| **Ar** | **$CH_2$** | **Me** | **Ar** | **$CH_2$** | **Me** | **Ar** | **$CH_2$** | **Me** |
| 47.16 | 45.11 | 46.61 | 46.04 | 43.23 | 42.66 | 45.35 | 42.41 | 43.22 |
| 101.05 | 101.87 | 105.17 | 100.29 | 100.37 | 101.21 | 99.24 | 99.55 | 102.16 |
| 156.90 | 159.97 | 163.72 | 156.50 | 158.87 | 159.76 | 155.09 | 158.06 | 161.11 |
| 205.60 | 207.27 | 197.93 | 205.52 | 206.49 | 193.98 | 203.79 | 205.68 | 195.54 |
| 251.70 | 253.22 | 252.53 | 251.92 | 252.75 | 248.58 | 249.89 | 251.93 | 250.50 |
| 296.51 | 293.08 | 299.25 | 297.02 | 292.89 | 295.29 | 294.70 | 292.07 | 297.52 |

| Conc. removed point 6/ mg/mL | | |
|---|---|---|
| **Ar** | **$CH_2$** | **Me** |
| 47.53 | 46.23 | 44.50 |
| 100.06 | 100.77 | 102.67 |
| 154.49 | 156.62 | 160.84 |
| 201.96 | 202.07 | 194.83 |
| 246.89 | 246.23 | 249.08 |
| 290.56 | 284.54 | 295.49 |

| | % RSD | | | |
|---|---|---|---|---|
| | **Ar** | **$CH_2$** | **Me** | |
| | 2.67 | 4.35 | 3.91 | |
| | 1.96 | 2.97 | 2.83 | |
| | 1.48 | 1.92 | 1.88 | |
| | 1.46 | 1.87 | 1.48 | |
| | 1.81 | 2.58 | 1.42 | |
| | 2.35 | 3.49 | 1.95 | |
| **AVERAGE** | 1.95 | 2.86 | 2.25 | = 2.35 |

*Table 5 Errors in MDMA calibration plots*

In this instance, it would appear the aromatic environment has lowest error, followed by Me and then $CH_2$. However, although it would seem fitting to simply use this environment for the qualitative and quantitative analysis of MDMA, the use of this peak must be used with caution. This is because, as seen in Figure 34, the aromatic protons are not simply an environment, but an ensemble of environments. It is therefore difficult to resolve individual $T_1$ values for the aromatic nuclei. This would suggest that the Me and $CH_2$ environment are more robust as they are singular environments. However, the appearance in the $^1H$ spectrum as a shoulder on the methyl peak due to stearate has been reported[76] and thus integrating this peak could be challenging. This would point to the $CH_2$ peak being the single best environment to use even though statistically it has the highest error. An additional reason to why this would be the best environment to use is the protons contained within the environment are not exchangeable protons. Therefore, the calculated integral should be accurate as they cannot be exchanged with solvent and should give a fairly accurate representation of how many protons are in the environment, thus enabling the concentration of MDMA in the sample to be determined.

There are several sources of error within the spectra themselves when integrating the proton environments in order to calculate the concentration of MDMA present in the sample. For example, it was seen with the $CH_2$ environment the signals were tailing and broadening as the MDMA concentration increased, meaning the ability to integrate became more challenging, therefore increasing the error associated with calculating the final concentration. Therefore, it should be noted the peaks cannot be integrated with exact confidence.

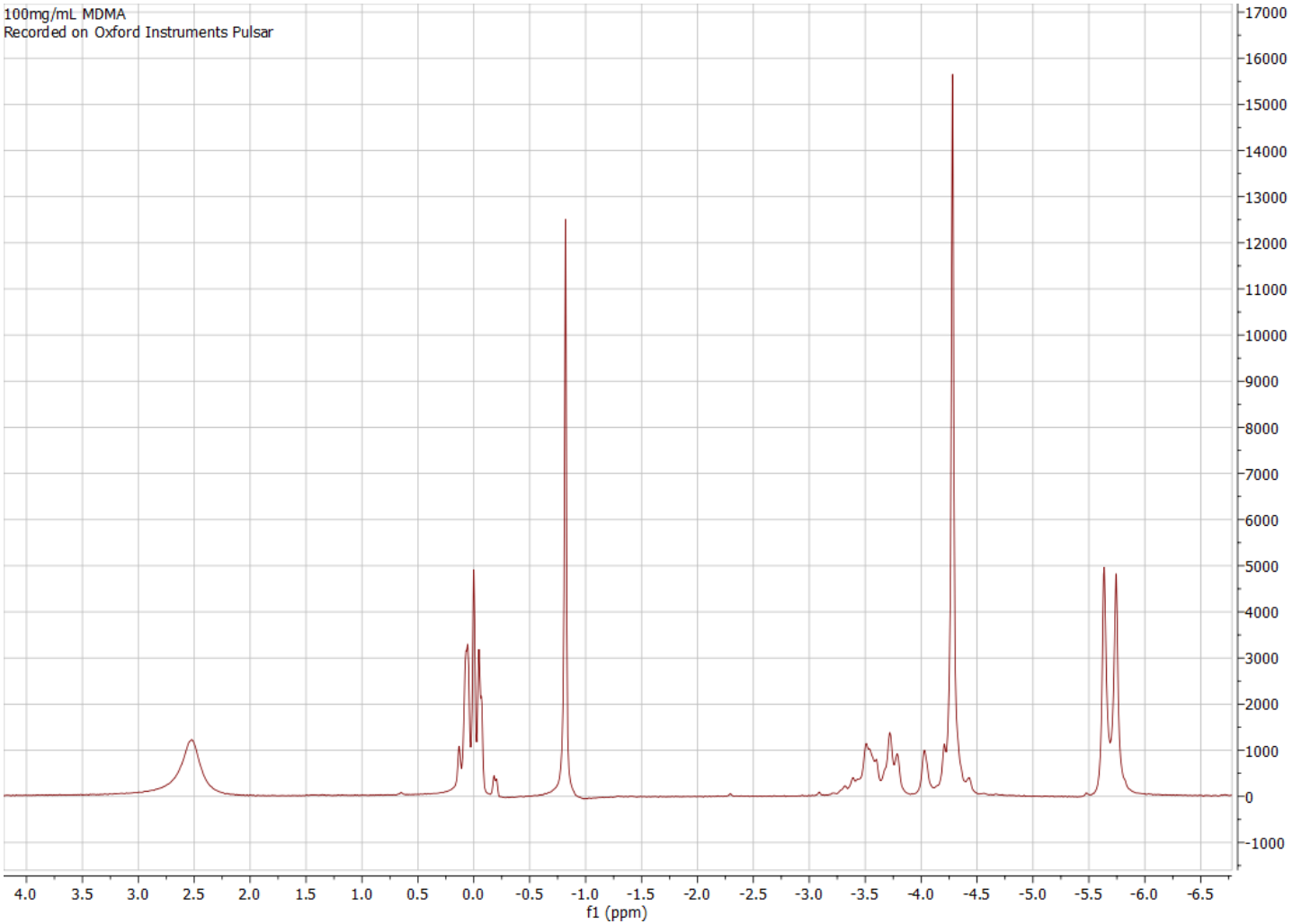


*Figure 34 100 mg/mL MDMA standard $^{1}H$ NMR spectrum*

## 4.6 Quantification of MDMA by GC-MS

### 4.6.1 GC-MS calibration

Similar to the NMR MDMA calibration curve, a calibration curve was produced using known MDMA standards in order to determine the concentration of MDMA present if found in suspected drug samples.

A calibration curve for MDMA (Figure 35) was obtained by performing GC analysis of samples of known concentrations, in this case 5 – 25 mg/mL of reference MDMA was used. Calibration standards were integrated and the peak area ratios (PARs) between MDMA and eicosane, which elute at retention times 5.634 and 7.234 minutes respectively. These were then used to construct calibration series, plotting PAR vs. increasing concentration. This produced a linear response ($y = 0.0747x + 0.2341$) with an $R^2$ of 0.995, thus showing good linearity. Using the calibration plot, it was possible to assess the quality of the calibration standards and the gradient of the plot would ultimately be used to calculate the concentration of MDMA in a sample by comparing the unknown, to a set of standard samples of known concentration.

| MDMA: 10 eico µg/mL | Peak Area MDMA | Peak Area Eicosane | Ratio Peak Area |
|---|---|---|---|
| MDMA 5 - 01 | 245.34 | 1230.24 | 0.1994 |
| MDMA 5 - 02 | 296.13 | 1463.36 | 0.2023 |
| MDMA 5 - 03 | 225.69 | 1289.09 | 0.1750 |
| MDMA 5 - 04 | 212.46 | 1157.58 | 0.1835 |
| MDMA 5 - 05 | 261.79 | 1284.81 | 0.2037 |
| MDMA 5 - 06 | 302.25 | 1669.33 | 0.1810 |
| MDMA 10 - 01 | 674.76 | 1525.71 | 0.4422 |
| MDMA 10 - 02 | 763.41 | 1612.31 | 0.4734 |
| MDMA 10 - 03 | 559.53 | 1101.66 | 0.5078 |
| MDMA 10 - 04 | 675.41 | 1357.3 | 0.4976 |
| MDMA 10 - 05 | 692.69 | 1354.85 | 0.5112 |
| MDMA 10 - 06 | 745.12 | 1619.35 | 0.4601 |
| MDMA 15 - 01 | 1242.93 | 1367.37 | 0.9089 |
| MDMA 15 - 02 | 1369.01 | 1617.71 | 0.8462 |
| MDMA 15 - 03 | 1295.42 | 1554.61 | 0.8332 |
| MDMA 15 - 04 | 1139.14 | 1170.99 | 0.9728 |
| MDMA 15 - 05 | 1077.1 | 1161.03 | 0.9277 |
| MDMA 15 - 06 | 944.28 | 1148.64 | 0.8220 |
| MDMA 20 - 01 | 2475.85 | 2392.18 | 1.0349 |
| MDMA 20 - 02 | 1785.25 | 1223.08 | 1.4596 |
| MDMA 20 - 03 | 1577.12 | 1402.59 | 1.1244 |
| MDMA 20 - 04 | 1689.57 | 1322.27 | 1.2777 |
| MDMA 20 - 05 | 2025.14 | 1659.92 | 1.2200 |
| MDMA 20 - 06 | 2128.62 | 1576.49 | 1.3502 |
| MDMA 25 - 01 | 3525.66 | 1975.85 | 1.7843 |
| MDMA 25 - 02 | 3413.98 | 2035.12 | 1.6775 |
| MDMA 25 - 03 | 3453.83 | 2038.65 | 1.6941 |
| MDMA 25 - 04 | 3787.81 | 2379.46 | 1.5918 |
| MDMA 25 - 05 | 3580.27 | 2006.76 | 1.7841 |
| MDMA 25 - 06 | 3082.34 | 1840.88 | 1.6743 |

| MDMA: 10 eico µg/mL | Av. Peak Area |
|---|---|
| MDMA 5 | 0.1908 |
| MDMA 10 | 0.4821 |
| MDMA 15 | 0.8851 |
| MDMA 20 | 1.2445 |
| MDMA 25 | 1.7010 |

*Table 6 GC calibration table for MDMA over the range 5 - 25 mg/mL showing calculated peak area and average peak area*

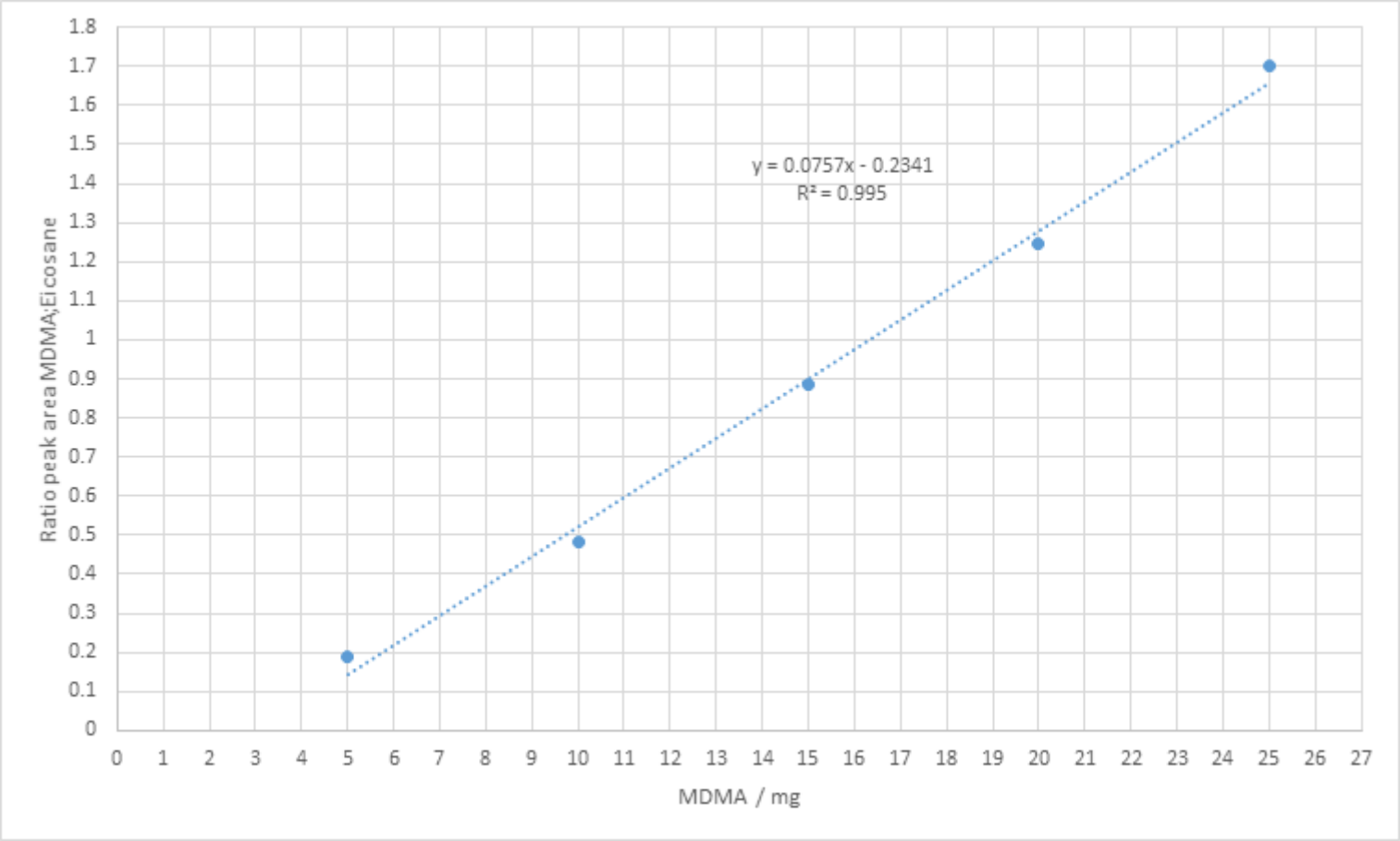


*Figure 35 GC calibration plot for MDMA over the range 5 - 25 mg/mL*

### 4.6.2 GC-MS Errors

Similar to the NMR calibration, the error was calculated for the GC calibration curve for MDMA. The graph produced had an $R^2$ of 0.9950, showing good linearity. Removal of each of the points allowed the error associated with this plot to be calculated and was found to be 2.52%. The result is given as a percentage relative standard deviation (%RSD). The %RSD calculated for the calibration graphs is approximately 3%, and therefore higher than that calculated for the NMR calibration curve. This would suggest the NMR method is more reproducible and would produce a more meaningful result with higher confidence than that of the GC.

Several sources of error associated with the method involve the integration method, as with the NMR method. With both the MDMA and eicosane peaks, the signals were tailing and broadening, and the baseline became noisier meaning the ability to integrate became more challenging. This would potentially, therefore, increase the error in calculating the peak area ratios for the spectrum, and ultimately is associated with calculating the final MDMA concentration.

Based on the errors associated with the measurements, both analytical methods can be compared due to their similar errors. It can also be seen that the difference in MDMA concentration calculated by both results is not due to the errors of the instruments.

## 4.7 MDMA Simulated Samples

Once calibration series was complete, simulated samples made up of a known concentration of MDMA were analysed to test the validity of the NMR method. Calcium carbonate ($CaCO_3$) was used as the filling agent as it is a common, insoluble filling agent generally utilised in the production of tablets. It therefore acts as an excipient that could potentially be part of an MDMA tablet. In this case, as an MDMA tablet is trying to be simulated so it can be analysed, it would be useful to use something insoluble that MDMA can hopefully be extracted from, without adulterating the product.

A known concentration of approximately 130 mg of MDMA per sample was used, so it was known what exact value was being sought after. This concentration was chosen as is close to the average found by EMCDDA, which reports an average of 125mg of MDMA per tablet.[75] Theoretically, each sample from the same batch should contain the same amount of MDMA per sample. The mean in this sample is 129.5 mg so there seems to be good uniformity and batch-to-batch variation is quite low. The error was calculated and was given as a percentage relative standard deviation (%RSD), in this case it was calculated to be 5.41% which equated to ± 7 mg of MDMA. So, the amount of MDMA in the sample is 129.5 mg ± 7 mg. As the amount of MDMA that is needed to produce a toxic response is 300 mg,[75] the method produced herein would be able to deduce this amount within acceptable limits.

## 4.8 Quantification of MDMA in seized sample

The quantification of MDMA in the 25 seized tablet samples of unknown identity were only attempted once the simulated samples quantified on the NMR had been proven to provide a successful result having been used on the model data. There is now a confidence that instrumental method is giving results which are in the right area with an acceptable level of error, so therefore it proves it is permitted to move onto unknowns and it will be possible to accurately determine MDMA concentrations and calculate errors.

### 4.8.1 NMR Results

The 25 suspected MDMA samples were photographed, homogenised and given a unique identifying number. 30 mg of the powder was removed, and the GC data was determined. The remainder of the powder was used to determine the MDMA concentration via $^{1}$H NMR. $^{1}$H NMR data were acquired first and the amount of MDMA found in the tablet samples ranged between 107.61 – 232.72 mg of MDMA per tablet. The mean value for the 25 samples was found to be 193.49 mg. This mean value is significantly higher than what was found by the EMDCCA, which reported an average of 125 mg MDMA per tablet.[75] The mean amount of MDMA found *via* NMR for the tablet samples is significantly higher than that reported by the EMCDDA. This would suggest the average content of MDMA in tablets has increased in recent years and the EMCDDA should potentially re-assess the average it reports.

The reason the average amount of MDMA may have increased in recent years could be due to the manufacturing process having an improved, increased yield, and therefore the purity of MDMA in the tablet is increased.[75] This may be due to the popularity of the use of the drug in its tablet form, as compared to the purer crystal MDMA which is simply a version of the drug without the addition of a filing agent, simply because it is easier to take. The prevalence of MDMA use may be an additional reason to why the average amount of the drug per tablet has increased. For example,

a recent report from a UK festival onsite drug checking service reported that the most common drug identified was MDMA, with a positive result of almost 60%.[76]

### 4.8.2 GC Results

The suspected drug samples were analysed both quantitatively and qualitatively using GC. Similar to the NMR quantitative method, the spectrum for the sample collected on the GC was compared to a reference spectrum available on the Cayman Chemical database,[70] and with close similarity it was proven the samples contained MDMA. Qualitative analysis was performed on all the samples containing MDMA and concentrations obtained were used to be compared to the concentrations of MDMA calculated for the same samples using the NMR analytical method.

### 4.8.3 Results Comparison

The results for the concentrations of MDMA found in the tablets samples for both analytical techniques were compared and contrasted. The GC method is considered to be an accurate representation of the concentration as it has previously been proven to be the most reliable technique, so the NMR data was compared to it. However, the error calculations for NMR and GC techniques, as described in sections 4.5.3 and 4.6.2 respectively, showed the NMR analytical technique had a lower error than that of the GC. This could be the explanation as to why the data values obtained when calculating the difference in MDMA concentrations obtained using both methods varied were inconsistently higher and lower, ranging from 2.20 to 45.91 mg difference between the two.

As presented on Table 7 overleaf, it is seen the GC data does not have good correlation with the NMR data across all the tablet samples, with varying underestimations and overestimations being calculated by the NMR relative to the GC. A possible reason for the underestimation of the NMR could be that MDMA was absorbed onto stearate that was taken out during the filtration process as certain

pigments could have been able to absorb MDMA better, so it was trapped in the filter. Also, the extraction process of the MDMA from the $d_6$-DMSO solvent was not optimised as an extraction efficiency was not conducted, it was simply assumed solubility of MDMA was good. However, it is possible that if there was too much MDMA in the sample, the $d_6$-DMSO could become saturated not all the compound would go into solution. This would result in some of the MDMA being filtered away from the sample, and not all the MDMA being extracted.

| Sample code | Tablet weight / mg | Crushed tablet weight / mg | Average amount of MDMA in tablet by GC / mg | Average amount of MDMA in tablet by NMR / mg | Difference in amount of MDMA / mg | Hit score from qualitative NMR analysis |
|---|---|---|---|---|---|---|
| PB02 | 380.3 | 353.5 | 214.227 | 198.537 | 15.689 | 0.958 |
| PB03 | 387.9 | 376.7 | 200.116 | 197.920 | 2.196 | 0.947 |
| PB04 | 383.2 | 376.4 | 220.108 | 216.102 | 4.006 | 0.955 |
| PB05 | 397.9 | 392.1 | 248.152 | 228.483 | 19.669 | 0.953 |
| PB06 | 376.9 | 372.2 | 230.070 | 212.103 | 17.966 | 0.945 |
| PB07 | 380.1 | 372.6 | 197.819 | 211.209 | 13.389 | 0.945 |
| PB08 | 361.4 | 355.0 | 186.310 | 190.219 | 3.908 | 0.955 |
| PB09 | 387.9 | 386.4 | 184.919 | 218.944 | 34.024 | 0.944 |
| PB10 | 379.6 | 371.0 | 181.765 | 215.524 | 33.759 | 0.946 |
| PB11 | 378.5 | 374.2 | 168.221 | 211.036 | 42.814 | 0.946 |
| PB12 | 388.5 | 378.0 | 174.852 | 214.563 | 39.710 | 0.944 |
| PB13 | 383.9 | 379.5 | 176.798 | 222.708 | 45.909 | 0.942 |
| PB14 | 370.2 | 361.8 | 183.421 | 205.439 | 22.017 | 0.945 |
| PB15 | 375.1 | 368.1 | 177.303 | 200.673 | 23.370 | 0.945 |
| PU01 | 450.4 | 439.0 | 118.735 | 107.610 | 11.124 | 0.953 |
| PR01 | 448.4 | 428.9 | 172.864 | 200.450 | 27.585 | 0.923 |
| PR02 | 443.4 | 424.7 | 171.707 | 181.369 | 9.661 | 0.934 |
| YR01 | 503.1 | 486.1 | 183.602 | 224.763 | 41.161 | 0.931 |
| BR01 | 484.4 | 473.2 | 122.933 | 141.800 | 18.866 | 0.945 |
| YS01 | 289.3 | 264.8 | 121.996 | 139.935 | 17.939 | 0.961 |
| WA01 | 390.1 | 369.5 | 141.403 | 178.850 | 37.447 | 0.948 |
| GS01 | 500.4 | 476.7 | 146.298 | 158.490 | 12.191 | 0.958 |
| RB01 | 603.8 | 585.4 | 166.264 | 196.668 | 30.403 | 0.931 |
| BT01 | 457.8 | 438.9 | 206.139 | 232.723 | 26.584 | 0.946 |
| GH01 | 252.5 | 239.7 | 126.733 | 131.189 | 4.455 | 0.962 |

*Table 7 Comparison of MDMA concentrations obtained by NMR and GC*

A possible reason for the overestimation of the concentration *via* NMR, or underestimation *via* GC, may be due to the solubility of MDMA being different in different solvents. This was due to both methods requiring different solvents in order to operate and carry out the analysis. Although the same tablet samples were analysed using both analytical methods, and the same concentrations of MDMA should have been expected, with the solvent being MeOH for the GC analysis and $d_6$-DMSO for the NMR analysis there is a possibility MDMA has a better solubility in MeOH. This would mean the solvent can take up more of the drug than $d_6$-DMSO, as it becomes saturated at a higher concentration. This may explain the variation in the MDMA concentration in the samples, calculated from both analytical techniques.

# 5 Conclusions

The results from the analysis of the tablet samples showed that they contained only MDMA, as they all had NMR hit scores of greater than 92.3% and had the same retention times when analysed using the GC, indicating no PMA was present. However, should such tablets come about, it would be possible to differentiate them and distinguish between both compounds due to their distinctly different peaks on their $^{1}H$ NMR spectra and different retention times on their GC chromatograms. IR spectroscopy, however, is not recommended for determining if a sample consists of MDMA, PMA or a combination. A detection method for MDMA was developed on the GC-MS using the calibration standards prepared and the graph produced from the results obtained from the method showed good linearity, with an $R^2$ value of 0.995, over the range of interest in relation to the concentration of MDMA present in the sample. This was then validated with a group of tablet samples containing MDMA and the results gave confidence in the method as the values obtained for the concentration of MDMA in the tablets was in line with the literature (EMCDDA). Therefore, the GC method developed could be used as a comparative method when developing an NMR method.

Focusing on three discrete proton environments, it was possible to successfully detect and quantify MDMA *via* NMR. In order to test the validity of the NMR method, simulated samples consisting of MDMA and $CaCO_3$ were tested. The results had low error, with the concentration of MDMA being calculated to have an average 0.5 mg difference to the expected value. The tablet samples used in the GC method were then analysed, and the outcome from the analysis showed the results for the concentration of MDMA in the tablets had a lower error than calculated on the GC. This would lead one to assume the NMR method has a higher accuracy and thus produces more reliable results. With the collection of the sample's NMR data and the subsequent analysis taking approximately only 5 minutes, the method was also proven to be rapid.

Once the validity of the method was tested, it was confirmed accurate enough to be used on real street samples. 25 samples were analysed. $^{1}$H NMR analysis revealed that the amount of MDMA found in the tablet samples ranged between 107.61 – 232.72 mg of MDMA per tablet. The mean value for the 25 samples was found to be 193.49 mg. Analysis by GC-MS returned the range of MDMA content in the 25 samples to be 118.74 to 248.15 mg. The mean value for the 25 samples was found to be 176.91 mg. Both mean values are significantly higher than what was found by the EMDCCA, which reported an average of 125 mg MDMA per tablet.[75] This would suggest the average content of MDMA in tablets has increased in recent years and the EMCDDA should potentially re-assess the average it reports. Comparison of the NMR and GC-MS values of determined MDMA content indicated a variance of 2.20 to 45.91 mg. This variance can partly be accounted for in terms of the difference in accuracy between the two methods, in that the GC-MS calibration plot possessed a higher RSD than the corresponding NMR plot (3.0% compared to 2.4%).

# 6 Future Work

This significant piece of research shows it is possible to both identify and quantify suspected drug tablet samples and an example of MDMA was the focus of this in this project. It has been proven that, in this instance, the method and technique by NMR was significantly better than the usual 'gold-standard' method of (GC) mass spectrometry.

This investigation could be extended to look at adulterated MDMA samples to see if it can accurately determine multi-component mixtures. None of the samples analysed in this investigation contained PMA but if it was an early preliminary investigation, preliminary results would indicate this approach could be used as there are discrete signals that could be investigated. For example, Figure 36 overleaf shows a simulated NMR spectrum showing what would be the outcome spectrum if a sample containing a mixture of MDMA and PMA was analysed. This can be used to validate samples as they do not contain the PMA peaks shown.

If the quantities of MDMA and PMA were to be calculated using this NMR technique, the signals to be used for the NMR quantification would likely be the $CH_2$ (methylene) and $OCH_3$ (methoxy). The aromatic region would likely not be used as the region is not viable, this is because in PMA the overlapping peaks would be difficult to distinguish, as within the combined spectrum. This shows that even though these samples do not contain PMA, it could be possible to distinguish mixed samples. If the technique works, due to the convenience of it, it could be used on different new/emerging drugs. The drug data base would only needed to be updated for new/emerging drugs however, otherwise the technique should be successful.

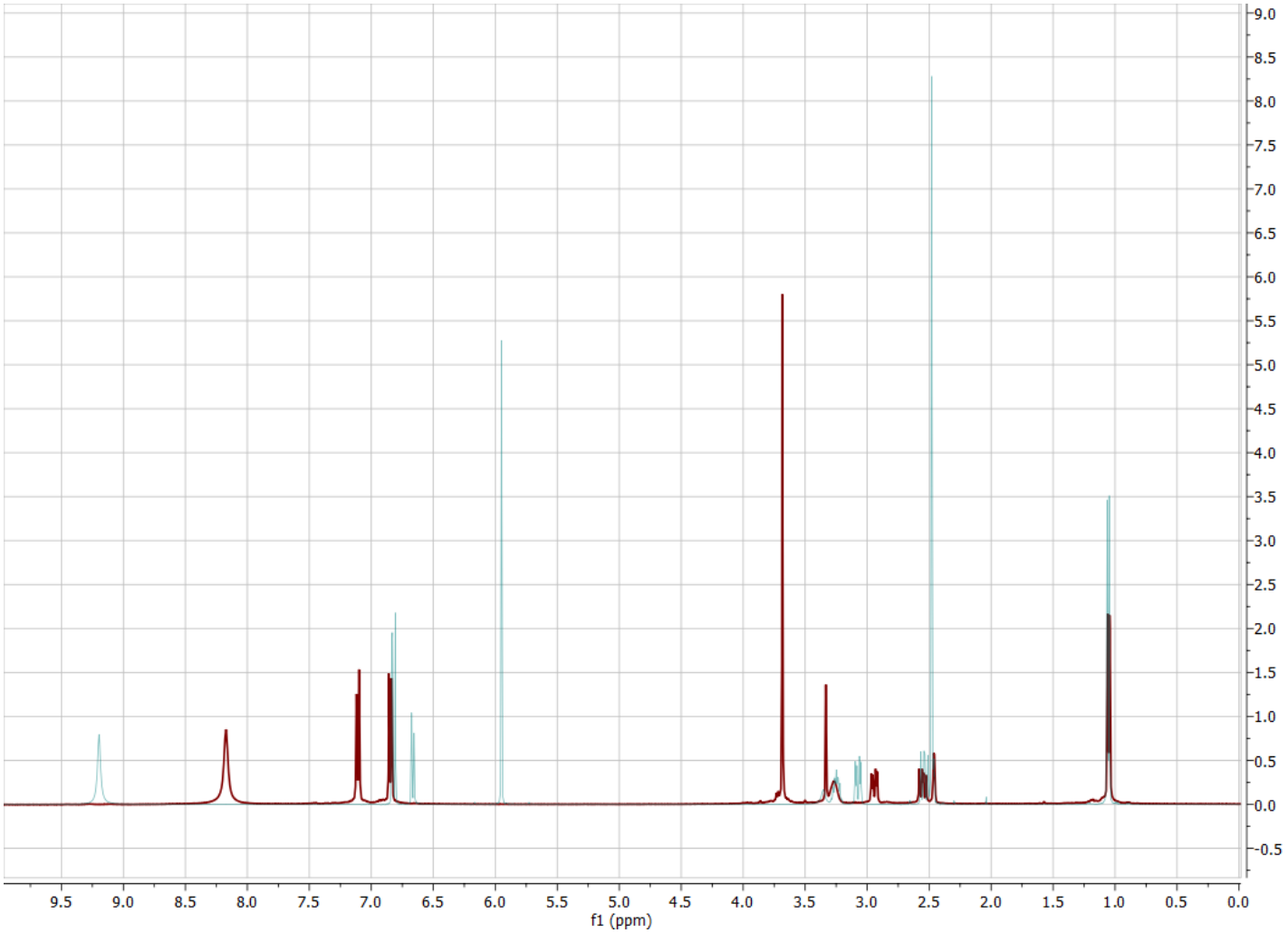


*Figure 36 Overlaid NMR spectra simulating a sample of MDMA (blue) adulterated with PMA (red).*

# 7 References


1. NIDA, 'Understanding Drug Use and Addiction', 2018 (accessed August 2019)
2. Healthline, 'The Most Addictive Prescription Drugs on the Market', 2018 (accessed August 2019)
3. S. Cortese, N. Adamo, C. Del Giovane, C. Mohr-Jensen, A. J. Hayes, S. Carucci, L. Z. Atkinson, L. Tessari, T. Banaschewski, D. Coghill, C. Hollis, E. Simonoff, A. Zuddas, C. Barbui, M. Purgato, H. C. Steinhausen, F. Shokraneh, J. Xia, A. Cipriani, *Lancet Psychiatry*, 2018, **5**, 727-738
4. N. S. Miller, R. B. Millman, M. S. Gold, *AASA*, 1989, **8**, 53 – 69
5. T. Steinkellner, M. Freissmuth, H. H. Sitte, T. Montgomery, *Bio Chem*, 2015, **392**, 103 – 115
6. R. Sinha, *Anna. NY. Acad. Sci*, 2009, **1141**, 105 – 130
7. T. R. Kosten, B. J. Rounsaville, H. D. Kleber, *Arch. Gen. Psychiatry*, 1986, **43**, 733 – 739
8. MedlinePlus, 'Substance use disorder', 2018 (accessed August 2019)
9. K. Moore, S. Miles, *Addiction Research*, 2004, **12**, 507 – 523
10. Home Office, 'Drug Misuse: Findings from the 2017/18 Crime Survey for England and Wales', 2018, (accessed August 2019)
11. Mirror, 'Inside the Parklife drugs lab where a 60 second test is saving lives', 2018 (accessed August 2019)
12. DrugWise, 'New psychoactive substances', 2018 (accessed August 2019)
13. H. Klee, P. Reid, *Health*, 1998, **2**, 115 – 134
14. ONS, 'Deaths of homeless people in England and Wales – local authority estimates: 2013 to 2017', 2019 (accessed August 2019)
15. H. Klee, P. Reid, *JCASP*, 2000, **10**, 69 – 75
16. H. Klee, P. Reid, *Health Soc Care Community*, 2002, **7**, 17 – 24
17. L. Jason-Lloyd, *Misuse of Drugs: A Straightforward Guide to the Law*, 2007, **7**, 6 – 7
18. nidirect, 'Drugs and crime' (accessed June 2019)
19. Release, 'Schedules', (accessed September 2019)

20. T. Bennett, K. Holloway, *Understanding Drugs, Alcohol and Crime*, 2005, **1**, 25
21. R. M. Baum, *C&EN*, 1985, **63**, 7
22. *OJ*, 2005, **127**, 32
23. L. A. King, *DTA*, 2011, **3**, 401 – 403
24. J. Nonnekes, B. Post, J. W. Tetrud, J. W. Langston, B. R. Bloem, *Lancet Neurol*, 2018, **17**, 300 – 301
25. G. L. Henderson, *JFS*, 1988, **33**, 569 – 575
26. D. A. Volpe, G. A. M. Tobin, R. D. Mellon, A. G. Katki, R. J. Parker, T. Colatsky, T. J. Tropp, S. L. Verbois, *Regul Toxicol Pharmacol*, 2011, **59**, 385 – 390
27. ADF, 'New psychoactive substances', 2019 (accessed August 2019)
28. F. I. Carroll, A. H. Lewin, S. W. Mascarella, H. H. Seltzman, P. A. Reddy, *Ann. N.Y. Acad. Sci.*, 2012, **1248**, 18 – 38
29. GOV, 'Psychoactive Substances Act 2016', 2015 (accessed August 2019)
30. Independent, 'Legal highs ban 'will increase drug-related deaths' by moving sales underground', 2016 (accessed August 2019)
31. L. H. Gold, G. F. Koob, M. A. Geyer, *JPET*, 1988, **247**, 547 – 555
32. ONS, 'Deaths related to drug poisoning in England and Wales: 2018 registrations', 2019 (accessed August 2019)
33. N. Solowij, W. Hall, N. Lee, *Br. J. Addict*., 1992, **87**, 1161 – 1172
34. M. E. Leichti, C. Baumann, A. Gamma, F. X. Vollenweider, *Neuropsychopharmacology*, 2000, **22**, 513 – 521
35. NIDA, 'What are the effects of MDMA?' (accessed June 2019)
36. R. H. Schwartz, N. S. Miller, *Pediatrics*, 1997, **100**, 705 – 708
37. A. Gamma, A. Buck, T. Berthold, M. E. Liechti, F. X. Vollenweider, D. Hell, *Neuropsychopharmacology*, 2000, **23**, 388 – 395
38. C. M. Hysek. Y. Schmid, L. D. Simmler, *Soc Cogn Affect Neurosci*, 2014, **9**, 1645 – 1652
39. D. Davidson, A. C. Parrott, *Hum Psychopharmacol*, 1997, **12**, 221 – 226
40. M. Mas, M. Farre, R. de la Torre, P. N. Roset, J. Ortuno, J. Segura, J. Cami, *JPET*, 1999, **290**, 136 – 145
41. G. D. van Dijken, R. E. Blom, R. J. Hene, W. H. Boer, *Nephrol Dial Transplant*, 2013, **28**, 2277 – 2283

42. G. A. Campbell, M. H. Rosner, *CJASN*, 2003, **3**, 1852 – 1860
43. S. Droogmans, B. Cosyns, H. D'haenen, *Am. J. Cardiol*, 2007, **100**, 1442 – 1445
44. Drugs, 'PMA/PMMA harm reduction information', (accessed October 2019)
45. S. Refstad, *AAS*, 2003, **47**, 1298 – 1299
46. I. D. Montoya, D. J. McCann, *EXS*, 2010, **100**, 519 – 541
47. A. Suvanujasiri, J. Holloman, S. Sinha, T. Nephew, M. LaChance, T. Kifle, H. Kyeyune, D. Stewart, *NASATS*, 2016, **1**, 2 – 9
48. T. L. Anderson, *Enc. Cri*, 2001, **4**, 286 – 289
49. N. Krone, B. A. Hughes, G. G. Lavery, P. M. Stewart, W. Arlt, C. H. L. Shackleton, *J Steroid Biochem Mol Biol*, 2010, **121**, 496 – 504
50. J. L. Valentine, R. Middleton, *J. Anal. Toxicol*, 2000, **24**, 211 – 222
51. J. M. Halket, D. Waterman, A. M. Przyborowska, R. K. P. Patel, P. D. Fraser, P. M. Bramley, *J. Exp. Bot*, 2005, **56**, 219 – 243
52. S. B. Teich, M. C. Slusher, *Physics Today*, 1992, **45**, 87 – 88
53. J. A. Ryan, S. V. Compton, M. A. Brooks, D. A. C. Compton, *J Pharm Biomed Anal*, 1991, **9**, 303 – 310
54. S. H. Scafi, C. Pasquini, *RSC Adv*, 2001, **126**, 2218 – 2224
55. L. A. C. Pieters, A. J. Vlietinck, *J Pharm Biomed Anal*, 1989, **7**, 1405 – 1417
56. U. Holzgrabe, M. Malet-Martino, *J Pharm Biomed Anal*, 2011, **55**, 679 – 687
57. M. Malet-Martino, R. Martino, *eMagRes*, 2015, 4
58. A. D. Gossert, W. Jahnke, *Prog Necl Mag Res Sp*, 2016, **97**, 82 – 125
59. Y. Zhong, K. Huang, Q. Luo, S. Yao, X. Liu, N. Yang, C. Lin, X. Luo, I*nt. J. Anal. Chem*, 2018, **2018**, 1 – 7
60. G. F. Pauli, S. N. Chen, C. Simmler, D. C. Lankin, T. Gödecke, B. U. Jaki, J. B. Friesen, J. B. McAlpine, J. G. Napolitano, *J. Med. Chem*, 2014, **57**, 9220 – 9231
61. I. C. Jones, G. J. Sharman, J. Pidgeon, *MRC*, 2005, **43**, 497 – 509
62. E. M. Lenz, D. Greatbanks, I. D, Wilson, M. Spraul, M. Hofmann, J. Troke, J. C. Lindon, J. K. Nicholson, *Anal. Chem*., 1996, **68**, 2832 - 2837
63. H. A. Naqi, S. M. Husbands, I. S. Blagbrough, *Anal Methods*, 2019, **11**, 4795 - 4807
64. D. B. G. Williams, M. Lawton, *J. Org. Chem*, 2010, **75**, 8351 – 8354

65. H. A. Buchanan, N. N. Daéid, W. Meier-Augenstein, H. F. Kemp, W. J. Kerr, M. Middleditch, *Anal. Chem*, 2008, **80**, 3350 – 3356
66. J. T. Liu, M. P. Sun, Y. S. Tsai, *JFS*, 2003, **2**, 59 – 68
67. A. Dobzhenetskiy, C. A. Gater, A. T. M. Wilcock, S. K. Langley, R. M. Brignall, D. C. Williamson, R. E. Mewis, *BJSE*, 2019, **28**, 339 – 347
68. D. A. Armbruster, T. Pry, *The Clinical Biochemist Reviews*, 2008, **29**, 49 – 52
69. M. Welvaert, Y. Rosseel, *PLoS One*, 2013, 8
70. Cayman Chemical, '3,4-MDMA (hydrochloride)' (accessed August 2019)
71. Cayman Chemical, '4-Methoxyamphetamine (hydrochloride)' (accessed August 2019)
72. D. J. Bell, J. Jones, Radiopaedia, '$T_1$ Relaxation time' (accessed August 2019)
73. R. S. Balaban, D. C. Peters, *JCMR*, 2010, **2**, 3 – 18
74. G. E. Murch, *Enc. Mat. Sci. Tech*, 2001, **2**, 2170 – 2176
75. J. Mounteney, A. Bo, A. Cunningham, I. Giraudon, J. Matias, A. Pirona, N. van Gelder, A. Rybarska, L. Vandam, P. Griffiths, *EMCDDA*, 2016, **1**, 7
76. L. H. Antonides. R. M. Brignall, A. Costello, J. Ellison, S. E. Firth, N. Gilbert, B. J. Groom, S. J. Hudson, M. C. Hulme, J. Marron, Z. A. Pullen, T. B. R. Robertson, C. J. Schofield, D. C. Williamson, E. K. Kemsley, O. B. Sutcliffe, R. E. Mewis, *ACS Omega*, 2019, **4**, 7103−7112